Chapter 17. Aerotriangulation

17-1. Introduction

- *Aerotriangulation* is the term most frequently applied to the process of determining the $X, Y,$ and Z ground coordinates of individual points based on photo coordinate measurements
- *Phototriangulation* is perhaps a more general term, however, because the procedure can be applied to terrestrial photos as well as aerial photos
- With improved photogrammetric equipment and techniques, accuracies to which ground coordinates can be determined by these procedures have become very high
- One of the principal applications lies in extending or densifying ground control through strips and/or blocks of photos for use in subsequent photogrammetric operations
- When used for this purpose, it is often called ***bridging***, because in essence a "bridge" of intermediate control points is developed between field-surveyed control that exists in only a limited number of photos in a strip or block

17-1. Introduction

- Establishment of the needed control for compilation of topographic maps with stereoplotters is an excellent example to illustrate the value of aerotriangulation
- In this application, the practical minimum number of control points necessary in each stereomodel is three horizontal and four vertical points
- For large mapping projects, therefore, the number of control points needed is extensive, and the cost of establishing them can be extremely high if it is done exclusively by field survey methods
- Much of this needed control is now routinely being established by aerotriangulation from only a sparse network of field-surveyed ground control and at a substantial cost savings
- A more recent innovation involves the use of kinematic GPS and INS in the aircraft to provide coordinates and angular attitude of the camera at the instant each photograph is exposed
- In theory, this method can eliminate the need for ground control entirely, although in practice a small amount of ground control is still used to strengthen the solution

17-1. Introduction

❖ Besides having an economic advantage over field surveying, aerotriangulation has other benefits:

(1) most of the work is done under laboratory conditions, thus minimizing delays and hardships due to adverse weather conditions

(2) access to much of the property within a project area is not required

(3) field surveying in difficult areas, such as marshes, extreme slopes, and hazardous rock formations, can be minimized

(4) the accuracy of the field-surveyed control necessary for bridging is verified during the aerotriangulation process, and as a consequence, chances of finding erroneous control values after initiation of compilation are minimized and usually eliminated

17-1. Introduction

- Apart from bridging for subsequent photogrammetric operations, aerotriangulation can be used in a variety of other applications in which precise ground coordinates are needed although most of these uses have been largely supplanted by GPS
- In property surveying, aerotriangulation can be used to locate section corners and property corners or to locate evidence that will assist in finding these corners
- In topographic mapping, aerotriangulation can be used to develop digital elevation models by computing X, Y, and Z ground coordinates of a systematic network of points in an area, although airborne laser scanning is commonly being used for this task
- Aerotriangulation has been used successfully for densifying geodetic control networks in areas surrounded by tall buildings where problems due to multipath cause a loss of accuracy in GPS surveys
- Special applications include the precise determination of the relative positions of large machine parts during fabrication
- It had been found especially useful in such industries as shipbuilding and aircraft manufacture

17-1. Introduction

- Methods of performing aerotriangulation may be classified into one of three categories: *analog, semianalytical*, and *analytical*
- Early **analog** procedures involved manual interior, relative, and absolute orientation of the successive models of long strips of photos using stereoscopic plotting instruments having several projectors ⇨ This created long strip models from which coordinates of pass points could be read directly
- Later, universal stereoplotting instruments were developed which enabled this process to be accomplished with only two projectors
- **Semianalytical aerotriangulation** involves manual interior and relative orientation of stereomodels within a stereoplotter, followed by measurement of model coordinates
- Absolute orientation is performed numerically—hence the term **semianalytical aerotriangulation**
- **Analytical** methods consist of photo coordinate measurement followed by numerical interior, relative, and absolute orientation from which ground coordinates are computed
- Various specialized techniques have been developed within each of the three aerotriangulation categories

17-2. Pass Points for Aerotriangulation

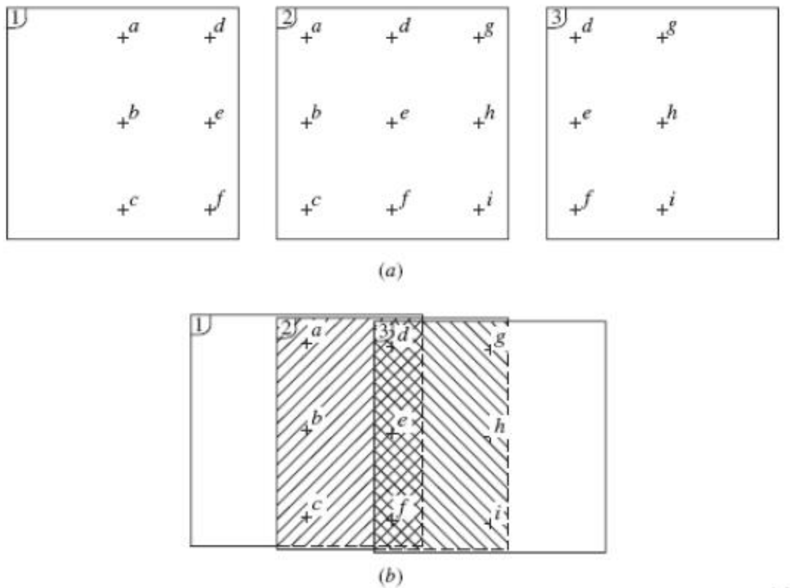

Figure 17-1. (a) Idealized pass point locations for aerotriangulation. (b) Locations of pass points in two adjacent stereomodels.

- ❖ Pass points for aerotriangulation are normally selected in the general photographic locations shown in Fig. 17-1a
- ❖ Historically, points were artificially generated using stereoscopic point marking devices
- ❖ These devices involved drilling a hole in the photograph, destroying the emulsion on that point
- ❖ Nowadays, in automatic aerotriangulation, pass points are usually found using automated procedures on digital and scanned-film photography
- ❖ Control points can be located manually with sub-pixel accuracy in software
- ❖ There is no destruction of the photograph using digital methods, so points can easily be removed and replaced

17-2. Pass Points for Aerotriangulation

- A typical procedure for measuring a pass point begins by first manually digitizing the point in one photograph
  - The pixels around this point serve as the template array
- Next, the user defines a search area in other photographs for automatic image matching
  - There are also automatic methods for defining a search area by predicting the coordinates of the point in the subsequent photographs
- Finally, the pixel patch in the search area corresponding to the template array is automatically located
  - Normalized cross-correlation followed by least squares matching is a common method for this step

17-2. Pass Points for Aerotriangulation

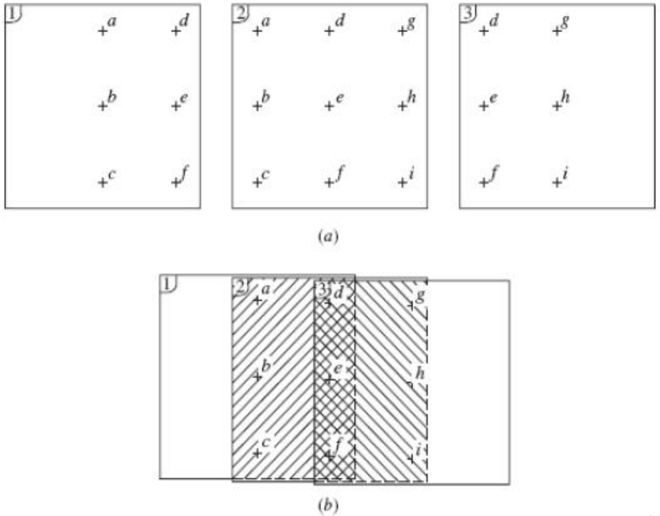

Figure 17-1. (a) Idealized pass point locations for aerotriangulation. (b) Locations of pass points in two adjacent stereomodels.

- To avoid poor matches and blunders, well-defined unique objects with good contrast and directionality should be selected as image-matching templates
- Image-matching software usually provides a measure of how well the point was matched, such as the correlation coefficient in normalized cross-correlation
  - ⇨ This number should serve as a guide for the user to decide whether or not to accept the matching results
- It is not uncommon for incorrectly matched points to have high correlation coefficients
- The process is repeated for each pass point keeping in mind the optimal distribution illustrated in Fig. 17-1
- Due to increased redundancy, the most effective points are those that appear in the so-called *tri-lap* area, which is <u>the area included on three consecutive images along a strip</u>
- Once many pass points are located, more can be added in a fully automated process by prediction of point locations based on a coordinate transformation

17-3. Fundamentals of Semianalytical Aerotriangulation

- Semianalytical aerotriangulation, often referred to as *independent model aerotriangulation*, is a partly analytical procedure that emerged with the development of computers
- It <u>involves relative orientation of each stereomodel of a strip or block of photos</u>
- After the models have been formed, they are numerically adjusted to the ground system by either a sequential or a simultaneous method
- In the sequential approach, contiguous models are joined analytically, one by one, to form a continuous strip model, and then absolute orientation is performed numerically to adjust the strip model to ground control
- In the simultaneous approach, all models in a strip or block are joined and adjusted to ground control in a single step, much like the simultaneous transformation technique

17-3. Fundamentals of Semianalytical Aerotriangulation

- An **advantage** of using semianalytical aerotriangulation is that independent stereomodels are more convenient for operators in production processes
- This stems from the fact that the images that make up stereomodel are more "tightly" oriented with respect to each other, whereas in fully analytical adjustments the images are oriented to optimize their fit with respect to a block of multiple photos which may lead to residual y parallax in the orientation between individual stereopairs
- Regardless of whether the sequential or simultaneous method is employed, the process yields coordinates of the pass points in the ground system
- Additionally, coordinates of the exposure stations can be determined in either process
  - ⇨ Thus, semianalytical solutions can provide initial approximations for a subsequent bundle adjustment

17-4. Sequential Construction of a Strip Model from Independent Models

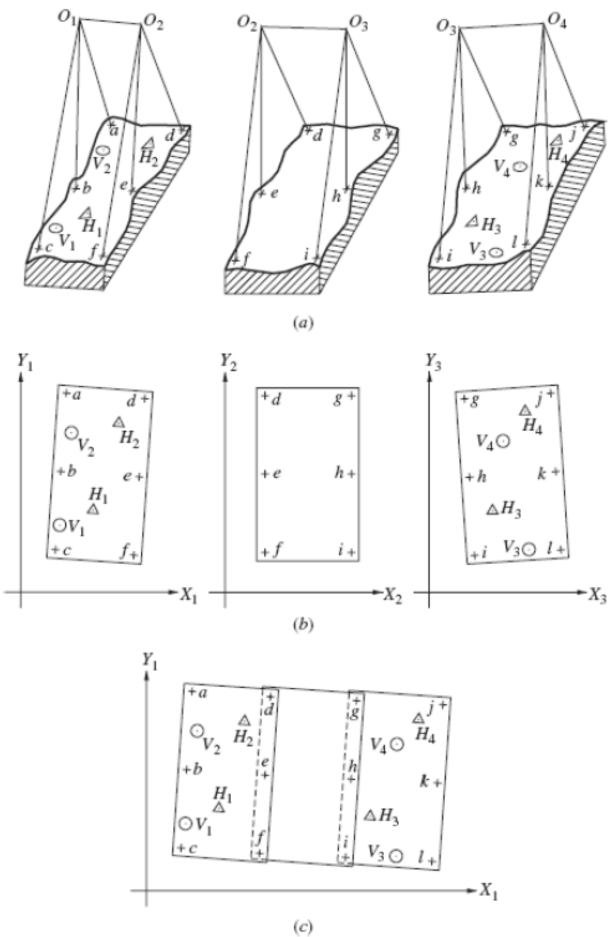

Figure 17–2. Independent model or semianalytical aerotriangulation. (a) Three adjacent relatively oriented stereomodels. (b) Individual arbitrary coordinate systems of three adjacent stereomodels. (c) Continuous strip of stereomodels formed by numerically joining the individual arbitrary coordinate systems into one system.

- In the sequential approach to semianalytical aerotriangulation, each stereopair of a strip is relatively oriented in a stereoplotter, the coordinate system of each model being independent of the others
- When relative orientation is completed, model coordinates of all control points and pass points are read and recorded
- This is done for each stereomodel in the strip. Figures 17-2a and b illustrate the first three relatively oriented stereomodels of a strip and show plan views of their respective independent coordinate systems

17-4. Sequential Construction of a Strip Model from Independent Models

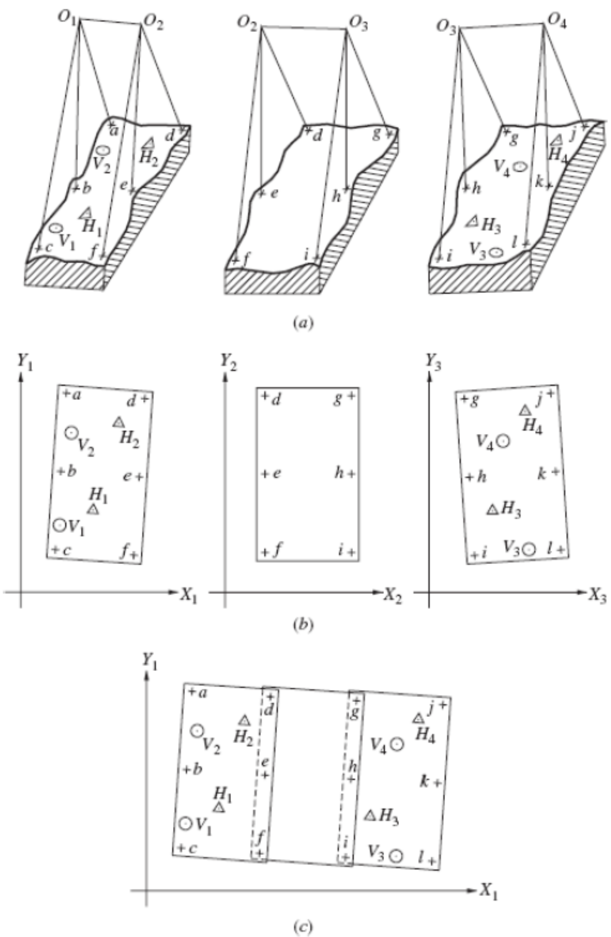

Figure 17–2. Independent model or semianalytical aerotriangulation. (a) Three adjacent relatively oriented stereomodels. (b) Individual arbitrary coordinate systems of three adjacent stereomodels. (c) Continuous strip of stereomodels formed by numerically joining the individual arbitrary coordinate systems into one system.

- ❖ By means of pass points common to adjacent models, a three-dimensional conformal coordinate transformation is used to tie each successive model to the previous one
- ❖ To gain needed geometric strength in the transformations, the coordinates of the perspective centers (model exposure stations) are also measured in each independent model and included as common points in the transformation
  - ❖ The right exposure station of model 1-2, O_2, for example, is the same point as the left exposure station of model 2-3. To transform model 2-3 to model 1-2, therefore, coordinates of common points $d, e, f,$ and O_2 of model 2-3 are made to coincide with their corresponding model 1-2 coordinates

17-4. Sequential Construction of a Strip Model from Independent Models

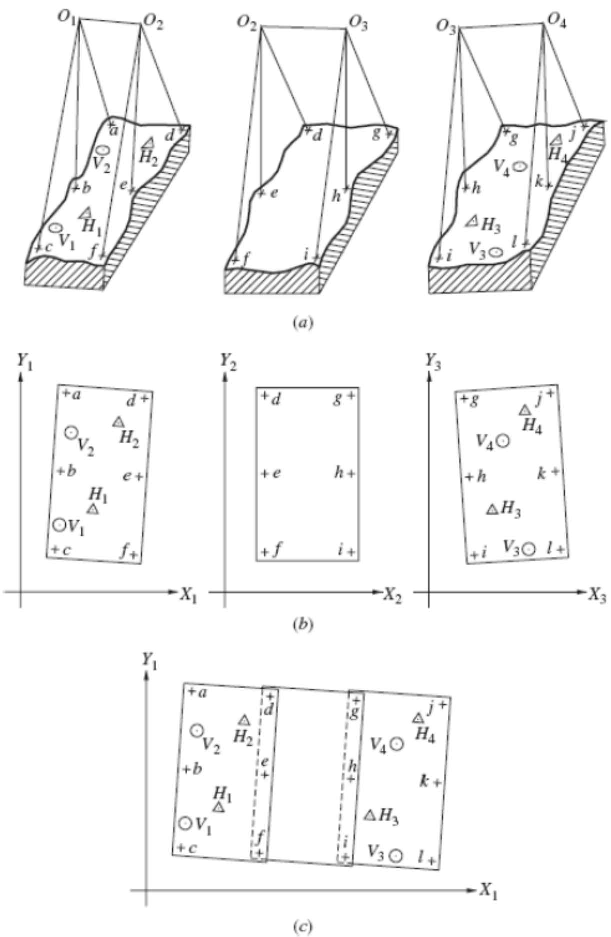

Figure 17–2. Independent model or semianalytical aerotriangulation. (a) Three adjacent relatively oriented stereomodels. (b) Individual arbitrary coordinate systems of three adjacent stereomodels. (c) Continuous strip of stereomodels formed by numerically joining the individual arbitrary coordinate systems into one system.

❖ Once the parameters for this transformation have been computed, they are applied to the coordinates of points $g, h, i,$ and O_3 in the system of model 2-3 to obtain their coordinates in the model 1-2 system

❖ These points in turn become control for a transformation of the points of model 3-4

❖ By applying successive coordinate transformations, a continuous strip of stereomodels may be formed, as illustrated in Fig. 17-2c

❖ The entire strip model so constructed is in the coordinate system defined by model 1-2

17-4. Sequential Construction of a Strip Model from Independent Models

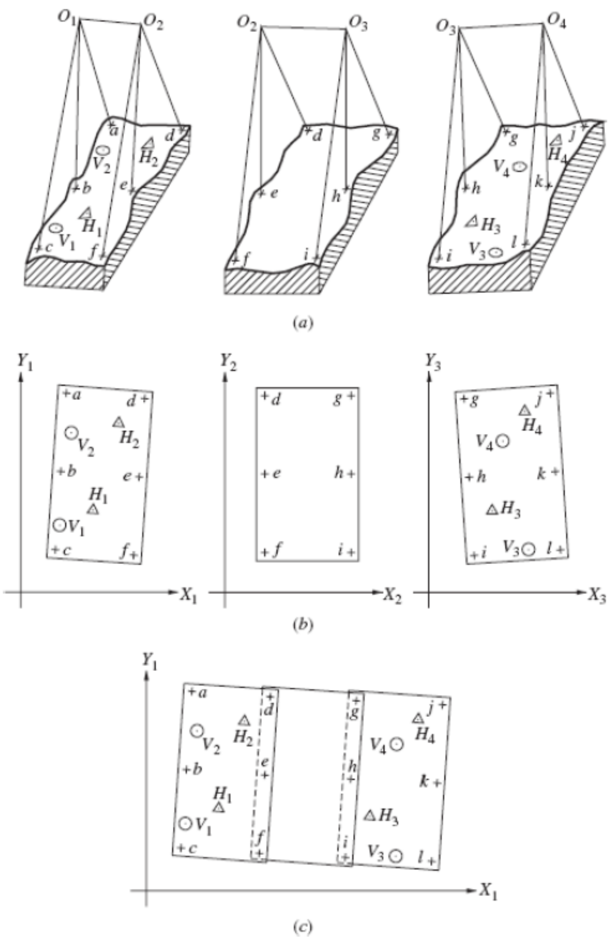

Figure 17–2. Independent model or semianalytical aerotriangulation. (a) Three adjacent relatively oriented stereomodels. (b) Individual arbitrary coordinate systems of three adjacent stereomodels. (c) Continuous strip of stereomodels formed by numerically joining the individual arbitrary coordinate systems into one system.

- Once the parameters for this transformation have been computed, they are applied to the coordinates of points g, h, i, and O in the system of model 2-3 to obtain their coordinates in the model 1-2 system
- These points in turn become control for a transformation of the points of model 3-4
- By applying successive coordinate transformations, a continuous strip of stereomodels may be formed, as illustrated in Fig. 17-2c
- The entire strip model so constructed is in the coordinate system defined by model 1-2

17-4. Sequential Construction of a Strip Model from Independent Models

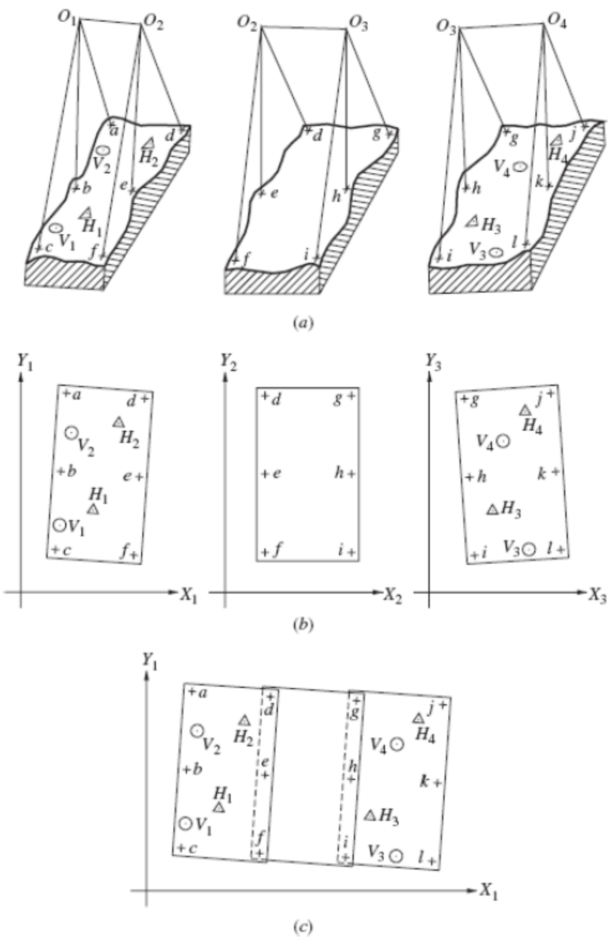

Figure 17–2. Independent model or semianalytical aerotriangulation. (a) Three adjacent relatively oriented stereomodels. (b) Individual arbitrary coordinate systems of three adjacent stereomodels. (c) Continuous strip of stereomodels formed by numerically joining the individual arbitrary coordinate systems into one system.

- Once the parameters for this transformation have been computed, they are applied to the coordinates of points g, h, i, and O in the system of model 2-3 to obtain their coordinates in the model 1-2 system
- These points in turn become control for a transformation of the points of model 3-4
- By applying successive coordinate transformations, a continuous strip of stereomodels may be formed, as illustrated in Fig. 17-2c
- The entire strip model so constructed is in the coordinate system defined by model 1-2

17-5. Adjustment of a Strip Model to Ground

- After a strip model has been formed, it is numerically adjusted to the ground coordinate system using all available control points
- If the strip is short, i.e., up to about four models, this adjustment may be done using a three-dimensional conformal coordinate transformation
- This requires that a minimum of two **horizontal control points** and three **vertical control points** be present in the strip
- More control than the minimum is desirable, however, as it adds stability and redundancy to the solution
- If the strip is long, a **polynomial adjustment** is preferred to transform model coordinates to the ground coordinate system

17-5. Adjustment of a Strip Model to Ground

❖ In the short strip illustrated in Fig. 17-2c, horizontal control points H_1 through H_4 and vertical control points V_1 through V_4 would be used in a three-dimensional conformal coordinate transformation to compute the ground coordinates of pass points a through l and exposure stations O_1 through O_4

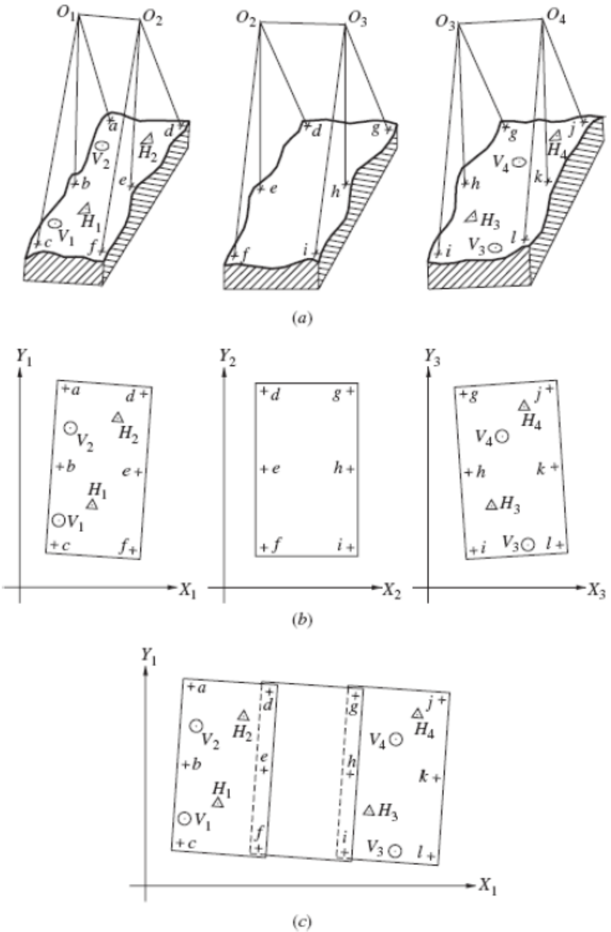

Figure 17–2. Independent model or semianalytical aerotriangulation. (a) Three adjacent relatively oriented stereomodels. (b) Individual arbitrary coordinate systems of three adjacent stereomodels. (c) Continuous strip of stereomodels formed by numerically joining the individual arbitrary coordinate systems into one system.

17-5. Adjustment of a Strip Model to Ground

❖ Due to the nature of sequential strip formation, random errors will accumulate along the strip

❖ Often, this accumulated error will manifest itself in a systematic manner with the errors increasing in a nonlinear fashion

❖ This effect, illustrated in Fig. 17-4, can be significant, particularly in long strips

❖ Figure 17-4a shows a strip model comprised of seven contiguous stereomodels from a single flight line

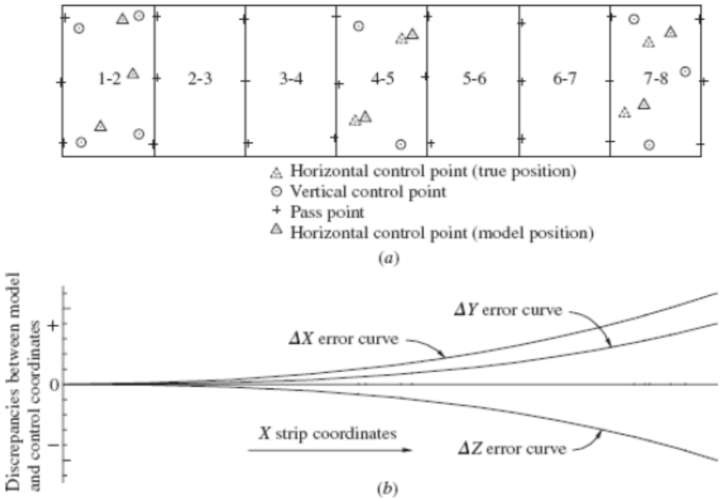

Figure 17-4. (a) Plan view of control extension of a seven-model strip. (b) Smooth curves indication accumulation of errors in X, Y, and Z coordinates during control extension of a strip.

❖ Note from the figure that sufficient ground control exists in model 1-2 to absolutely orient it (and thereby the entire strip) to the ground system

17-5. Adjustment of a Strip Model to Ground

❖ The **remaining control points** (in models 4-5 and 7-8) can then be used <u>as checkpoints to reveal accumulated errors along the strip</u>

❖ Figure 17-4b shows a plot of the discrepancies between model and ground coordinates for the checkpoints as a function of X coordinates along the strip

❖ Except for the ground control in the first model, which was used to absolutely orient the strip, discrepancies exist between model positions of horizontal and vertical control points and their corresponding field-surveyed positions

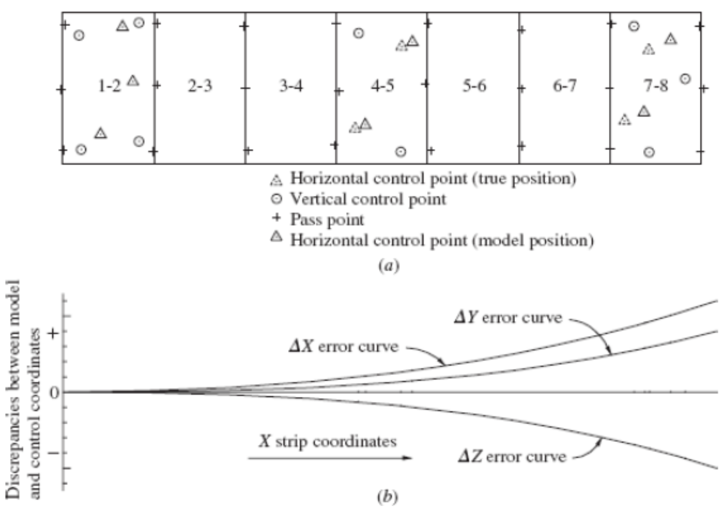

Figure 17-4. (a) Plan view of control extension of a seven-model strip. (b) Smooth curves indication accumulation of errors in X, Y, and Z coordinates during control extension of a strip.

❖ Smooth curves are fit to the discrepancies as shown in the figure

17-5. Adjustment of a Strip Model to Ground

- If sufficient control is distributed along the length of the strip, a **three-dimensional polynomial transformation** can be used in lieu of a conformal transformation to perform absolute orientation and thus obtain corrected coordinates for all pass points

- This polynomial transformation yields higher accuracy through modeling of systematic errors along the strip

- Most of the polynomials in use for adjusting strips formed by aerotriangulation are variations of the following third-order equations:

$$\begin{aligned}\bar{X} &= a_0 + a_1X + a_2Y + a_3X^2 + a_4XY + a_5Y^2 + a_6X^3 + a_7X^2Y + a_8XY^2 + a_9Y^3 \\ \bar{Y} &= b_0 + b_1X + b_2Y + b_3X^2 + b_4XY + b_5Y^2 + b_6X^3 + b_7X^2Y + b_8XY^2 + b_9Y^3 \\ \bar{Z} &= c_0 + c_1X + c_2Y + c_3X^2 + c_4XY + c_5Y^2 + c_6X^3 + c_7X^2Y + c_8XY^2 + c_9Y^3\end{aligned} \qquad (17\text{-}1)$$

- In Eqs. (17-1), $\bar{X}$, $\bar{Y}$ and $\bar{Z}$ are the transformed ground coordinates; X and Y are strip model coordinates; and the $a's$, $b's$, and $c's$ are coefficients which define the shape of the polynomial error curves. The equations contain 30 unknown coefficients ($a's, b's,$ and $c's$)

- Each three-dimensional control point enables the above three polynomial equations to be written, and thus 10 three-dimensional control points are required in the strip for an exact solution

17-5. Adjustment of a Strip Model to Ground

- When dealing with transformations involving polynomials, however, it is imperative to use redundant control which is well distributed throughout the strip
- It is important that the control points occur at the periphery as well, since extrapolation from polynomials can result in excessive corrections

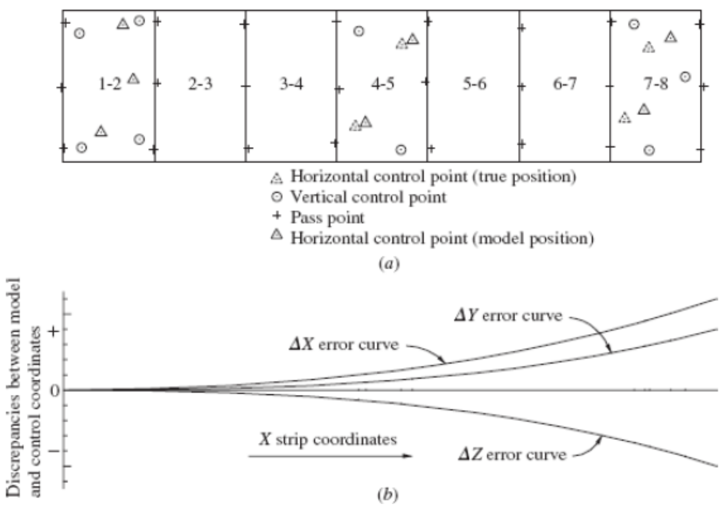

Figure 17–4. (a) Plan view of control extension of a seven-model strip. (b) Smooth curves indication accumulation of errors in X, Y, and Z coordinates during control extension of a strip.

- As illustrated by Fig. 17-4b, errors in X, Y, and Z are principally functions of the linear distance (X coordinate) of the point along the strip
- However, the nature of error propagation along strips formed by aerotriangulation is such that discrepancies in $X, Y,$ and Z coordinates are also each somewhat related to the Y positions of the points in the strip

17-5. Adjustment of a Strip Model to Ground

$$\begin{aligned}
\overline{X} &= a_0 + a_1X + a_2Y + a_3X^2 + a_4XY + a_5Y^2 + a_6X^3 + a_7X^2Y + a_8XY^2 + a_9Y^3 \\
\overline{Y} &= b_0 + b_1X + b_2Y + b_3X^2 + b_4XY + b_5Y^2 + b_6X^3 + b_7X^2Y + b_8XY^2 + b_9Y^3 \\
\overline{Z} &= c_0 + c_1X + c_2Y + c_3X^2 + c_4XY + c_5Y^2 + c_6X^3 + c_7X^2Y + c_8XY^2 + c_9Y^3
\end{aligned} \qquad (17\text{-}1)$$

- ❖ Depending on the complexity of the distortion, certain terms may be eliminated from Eqs. (17-1) if they are found not to be significant
- ❖ This serves to increase redundancy in transformation which generally results in more accurate results

17-6. Simultaneous Bundle Adjustment

- The most elementary approaches to analytical aerotriangulation consist of the same basic steps as those of analog and semianalytical methods and include
  (1) relative orientation of each stereomodel
  (2) connection of adjacent models to form continuous strips and/or blocks
  (3) simultaneous adjustment of the photos from the strips and/or blocks to field-surveyed ground control

- What is **different** about analytical methods is that the basic input consists of precisely measured photo coordinates of control points and pass points

- **Relative orientation** is then performed analytically based upon the measured coordinates and known camera constants

- Finally, the entire block of photographs is **adjusted simultaneously** to the ground coordinate system

17-6. Simultaneous Bundle Adjustment

- Analytical aerotriangulation tends to be more accurate than analog or semianalytical methods, largely because analytical techniques can more effectively eliminate systematic errors such as film shrinkage, atmospheric refraction distortions, and camera lens distortions
- In fact, X and Y coordinates of pass points can quite routinely be located analytically to an accuracy of within about 1/15,000 of the flying height, and Z coordinates can be located to an accuracy of about 1/10,000 of the flying height
- With specialized equipment and procedures, planimetric accuracy of 1/350,000 of the flying height and vertical accuracy of 1/180,000 have been achieved
- Another advantage of analytical methods is the freedom from the mechanical or optical limitations imposed by stereoplotters
- Photography of any focal length, tilt, and flying height can be handled with the same efficiency
- The calculations involved are rather complex
  - ⇨ however, a number of suitable computer programs are available to perform analytical aerotriangulation

17-6. Simultaneous Bundle Adjustment

- All different variations in analytical aerotriangulation techniques consist of writing condition equations that express the unknown elements of exterior orientation of each photo in terms of camera constants, measured photo coordinates, and ground coordinates
- The equations are solved to determine the unknown orientation parameters, and either simultaneously or subsequently, coordinates of pass points are calculated
- Analytical procedures have been developed which can simultaneously enforce collinearity conditions onto units which consist of hundreds of photographs
- The ultimate extension of the principles is to adjust all photogrammetric measurements to ground control values in a single solution known as a *bundle adjustment*
- The bundles from all photos are adjusted simultaneously so that corresponding light rays intersect at positions of the pass points and control points on the ground
- The process is an extension of the principles of analytical photogrammetry, applied to an unlimited number of overlapping photographs

17-6. Simultaneous Bundle Adjustment

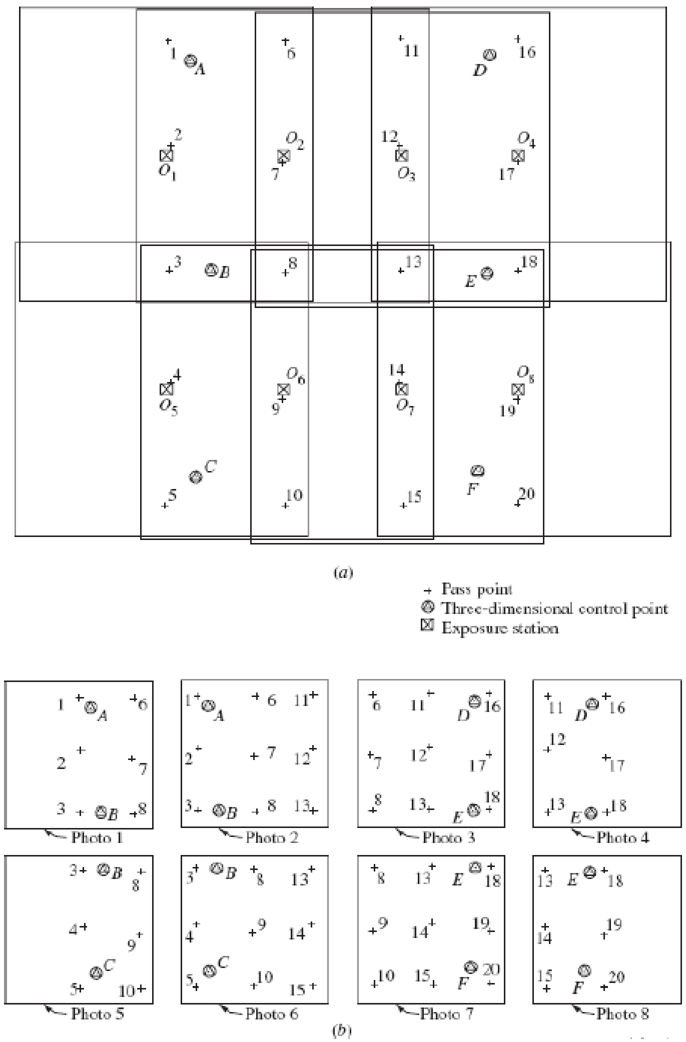

Figure 17-5. (a) Block of photos in overlapped position. (b) Separated photos showing image points.

- Figure 17-5a shows a small block consisting of two strips with four photos per strip
- The photo block contains images of 20 pass points labeled 1 through 20 and 6 control points labeled A through F, for a total of 26 object points
- Points 3, 8, 13, 18, B, and E also serve as *tie points* which connect the two adjacent strips
- Figure 17-5b shows the individual photos in a nonoverlapping configuration
- Note that photos 1, 4, 5, and 8 each contain images of 8 points; and photos 2, 3, 6, and 7 each contain images of 11 points, for a grand total of $4 \times 8 + 4 \times 11 = 76$ point images

17-6. Simultaneous Bundle Adjustment

❖ The unknown quantities to be obtained in a bundle adjustment consist of :
  (1) the X, Y, and Z object space coordinates of all object points
  (2) the exterior orientation parameters ($\omega, \varphi, \kappa, X_L, Y_L$, and Z_L) of all photographs

❖ The first group of unknowns (object space coordinates) is the necessary result of any aerotriangulation, analytical or otherwise

❖ Exterior orientation parameters, however, are generally not of interest to the photogrammetrist, but they must be included in the mathematical model for consistency

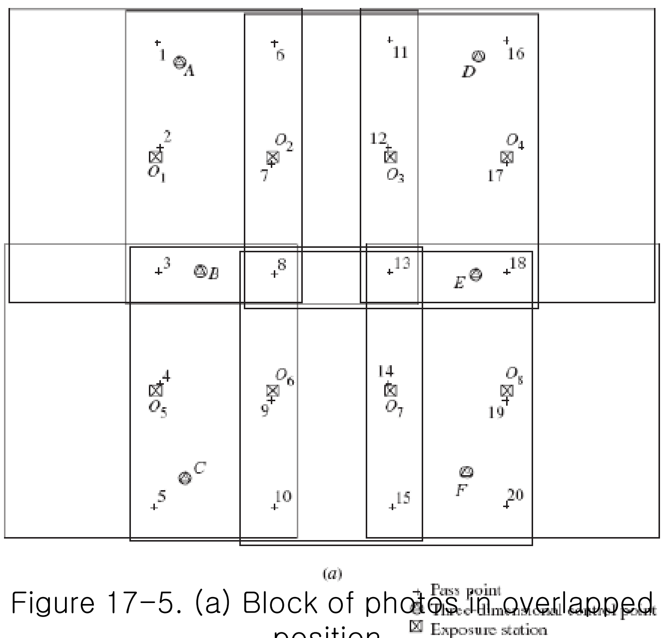

Figure 17–5. (a) Block of photos in overlapped position.

❖ In the photo block of Fig. 17-5a the number of unknown object coordinates is $26 \times 3 = 78$ (number of object points times the number of coordinates per point)

❖ The number of unknown exterior orientation parameters is $8 \times 6 = 48$ (number of photos times the number of exterior orientation parameters per photo) ⇨ Therefore the total number of unknowns is $78 + 48 = 126$

17-6. Simultaneous Bundle Adjustment

- The measurements (observed quantities) associated with a **bundle adjustment** are :
  - (1) x and y photo coordinates of images of object points
  - *(2)* $X, Y,$ and/or Z coordinates of ground control points
  - (3) direct observations of the exterior orientation parameters ($\omega, \varphi, \kappa, X_L, Y_L,$ and Z_L) of the photographs

- The first group of observations, photo coordinates, is the fundamental photogrammetric measurements
  - For a proper bundle adjustment they need to be weighted according to the accuracy and precision with which they were measured

- The next group of observations is coordinates of control points determined through field survey
  - Although ground control coordinates are indirectly determined quantities, they can be included as observations provided that proper weights are assigned

- The final set of observations, exterior orientation parameters, has recently become important in bundle adjustments with the use of airborne GPS control as well as *inertial navigation systems* (INSs) which have the capability of measuring the angular attitude of a photograph

17-6. Simultaneous Bundle Adjustment

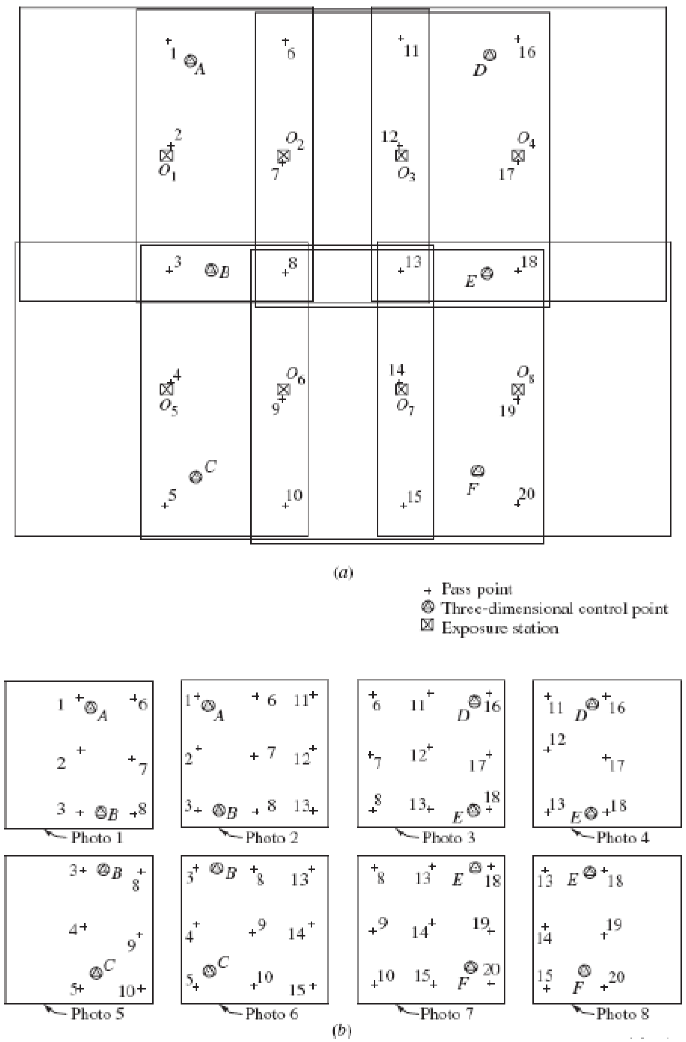

Figure 17-5. (a) Block of photos in overlapped position. (b) Separated photos showing image points.

- Returning to the block of Fig. 17-5, the number of photo coordinate observations is 76 × 2 = 152 (number of imaged points times the number of photo coordinates per point), and the number of ground control observations is 6 × 3 = 18 (number of three-dimensional control points times the number of coordinates per point)
- If the exterior orientation parameters were measured, the number of additional observations would be 8 × 6 = 48 (number of photos times the number of exterior orientation parameters per photo)

17-6. Simultaneous Bundle Adjustment

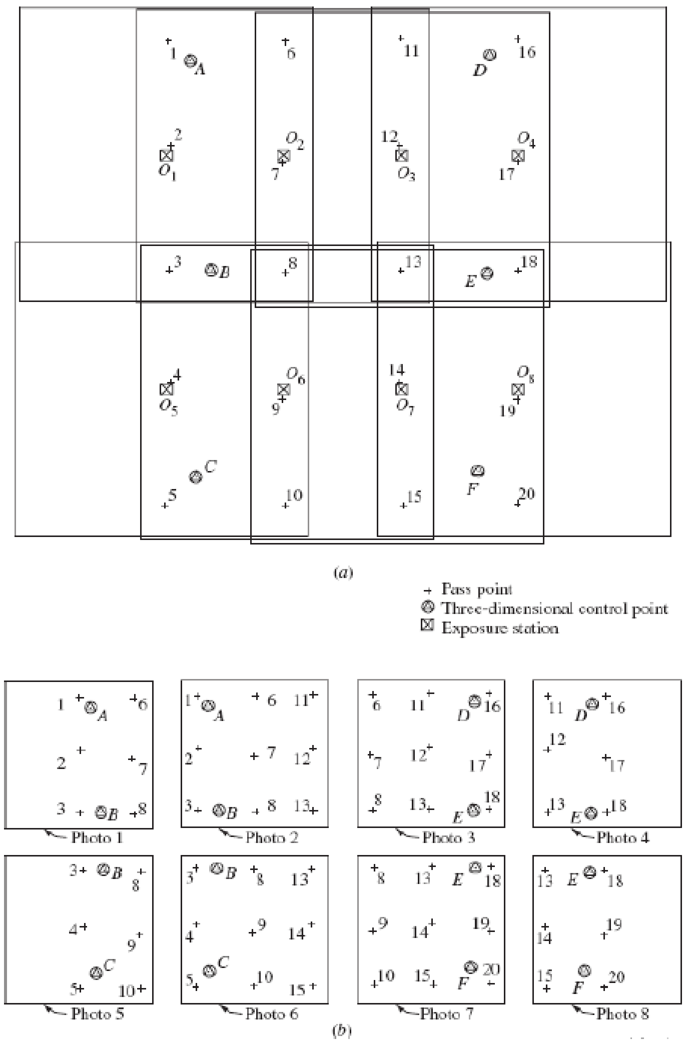

Figure 17-5. (a) Block of photos in overlapped position. (b) Separated photos showing image points.

- Thus, if all three types of observations are included, there will be a total of 152 + 18 + 48 = 218 observations; but if only the first two types are included, there will be only 152 + 18 = 170 observations

- Regardless of whether exterior orientation parameters were observed, a least squares solution is possible since the number of observations is greater than the number of unknowns (126) in either case

17-6. Simultaneous Bundle Adjustment

- The observation equations which are the foundation of a bundle adjustment are the collinearity equations

- These equations are given below in a slightly modified form as Eqs. (17-2) and (17-3)

$$x_{ij} = x_0 - f\left[\frac{m_{11_i}(X_j - X_{L_i}) + m_{12_i}(Y_j - Y_{L_i}) + m_{13_i}(Z_j - Z_{L_i})}{m_{31_i}(X_j - X_{L_i}) + m_{32_i}(Y_j - Y_{L_i}) + m_{33_i}(Z_j - Z_{L_i})}\right] \qquad (17\text{-}2)$$

$$y_{ij} = y_0 - f\left[\frac{m_{21_i}(X_j - X_{L_i}) + m_{22_i}(Y_j - Y_{L_i}) + m_{23_i}(Z_j - Z_{L_i})}{m_{31_i}(X_j - X_{L_i}) + m_{32_i}(Y_j - Y_{L_i}) + m_{33_i}(Z_j - Z_{L_i})}\right] \qquad (17\text{-}3)$$

- In these equations, $\boldsymbol{x_{ij}}$ and $\boldsymbol{y_{ij}}$ are the measured photo coordinates of the image of point $\boldsymbol{j}$ on photo $\boldsymbol{i}$ related to the fiducial axis system
  - x_0 and y_0 are the coordinates of the principal point in the fiducial axis system
  - f is the focal length (or more correctly, principal distance) of the camera
  - $m_{11_i}, m_{12_i}, \ldots, m_{33_i}$ are the rotation matrix terms for photo $\boldsymbol{i}$
  - X_j, Y_j, and Z_j are the coordinates of point j in object space
  - X_{Li}, Y_{Li}, and Z_{Li} are the coordinates of the incident nodal point of the camera lens in object space

17-6. Simultaneous Bundle Adjustment

❖ Since the collinearity equations are nonlinear, they are linearized by applying the first-order terms of Taylor's series at a set of initial approximations

➪ After linearization the equations can be expressed in the following matrix form:

$$\dot{B}_{ij}\dot{\Delta}_i + \ddot{B}_{ij}\ddot{\Delta}_j = \varepsilon_{ij} + V_{ij} \qquad (17\text{-}4)$$

where

$$\dot{B}_{ij} = \begin{bmatrix} b_{11_{ij}} & b_{12_{ij}} & b_{13_{ij}} & -b_{14_{ij}} & -b_{15_{ij}} & -b_{16_{ij}} \\ b_{21_{ij}} & b_{22_{ij}} & b_{23_{ij}} & -b_{24_{ij}} & -b_{25_{ij}} & -b_{26_{ij}} \end{bmatrix}$$

$$\ddot{B}_{ij} = \begin{bmatrix} b_{14_{ij}} & b_{15_{ij}} & b_{16_{ij}} \\ b_{24_{ij}} & b_{25_{ij}} & b_{26_{ij}} \end{bmatrix}$$

$$\dot{\Delta}_i = \begin{bmatrix} d\omega_i \\ d\phi_i \\ d\chi_i \\ dX_{L_i} \\ dY_{L_i} \\ dZ_{L_i} \end{bmatrix} \qquad \ddot{\Delta}_j = \begin{bmatrix} dX_j \\ dY_j \\ dX_j \end{bmatrix} \qquad \varepsilon_{ij} = \begin{bmatrix} J_{ij} \\ K_{ij} \end{bmatrix} \qquad V_{ij} = \begin{bmatrix} v_{x_{ij}} \\ v_{y_{ij}} \end{bmatrix}$$

- Matrix $\dot{B}_{ij}$ contains the partial derivatives of the collinearity equations with respect to the exterior orientation parameters of photo i, evaluated at the initial approximations
- Matrix $\ddot{B}_{ij}$ contains the partial derivatives of the collinearity equations with respect to the object space coordinates of point j, evaluated at the initial approximations
- Matrix $\dot{\Delta}_i$ contains corrections for the initial approximations of the exterior orientation parameters for photo i, and matrix $\ddot{\Delta}_j$ contains corrections for the initial approximations of the object space coordinates of point j
- Matrix ε_{ij} contains measured minus computed x and y photo coordinates for point j on photo i, and finally matrix V_{ij} contains residuals for the x and y photo coordinates

17-6. Simultaneous Bundle Adjustment

- Proper weights must be assigned to photo coordinate observations in order to be included in the bundle adjustment

- Expressed in matrix form, the weights for x and y photo coordinate observations of point j on photo i are :

$$W_{ij} = \sigma_0^2 \begin{bmatrix} \sigma_{x_{ij}}^2 & \sigma_{x_{ij}y_{ij}} \\ \sigma_{y_{ij}x_{ij}} & \sigma_{y_{ij}}^2 \end{bmatrix}^{-1} \qquad (17\text{-}5)$$

  - where σ_0^2 is the reference variance; $\sigma_{x_{ij}}^2$ and $\sigma_{y_{ij}}^2$ are variances in x_{ij} and y_{ij}
  - $\sigma_{x_{ij}y_{ij}}=\sigma_{y_{ij}x_{ij}}$ is the covariance of x_{ij} with y_{ij}

- The reference variance is an arbitrary parameter which can be set equal to 1, and in many cases, the covariance in photo coordinates is equal to zero
  - ⇨ In this case, the weight matrix for photo coordinates simplifies to

$$W_{ij} = \begin{bmatrix} \frac{1}{\sigma_{x_{ij}}^2} & 0 \\ 0 & \frac{1}{\sigma_{y_{ij}}^2} \end{bmatrix} \qquad (17\text{-}6)$$

- The next type of observation to be considered is ground control, and observation equations for ground control coordinates are

$$\begin{aligned} X_j &= X_j^{00} + v_{X_j} \\ Y_j &= Y_j^{00} + v_{Y_j} \\ Z_j &= Z_j^{00} + v_{Z_j} \end{aligned} \qquad (17\text{-}7)$$

  - where X_j , Y_j , and Z_j are unknown coordinates of point j,
  - X_j^{00}, Y_j^{00} and Z_j^{00} are the measured coordinate values for point j
  - v_{X_j}, v_{Y_j} and v_{Z_j} are the coordinate residuals for point j

17-6. Simultaneous Bundle Adjustment

❖ Even though ground control observation equations are linear, in order to be consistent with the collinearity equations, they will also be approximated by the first-order terms of Taylor's series

$$\begin{aligned} X_j^0 + dX_j &= X_j^{00} + v_{X_j} \\ Y_j^0 + dY_j &= Y_j^{00} + v_{Y_j} \\ Z_j^0 + dZ_j &= Z_j^{00} + v_{Z_j} \end{aligned} \qquad (17\text{-}8)$$

- X_j^0, Y_j^0 and Z_j^0 are initial approximations for the coordinates of point j
- dX_j, dY_j, and dZ_j are corrections to the approximations for the coordinates of point j

❖ Rearranging the terms of Eq. (17-8) and expressing the result in matrix form gives

$$\ddot{\Delta}_j = \ddot{C}_j + \ddot{V}_j \qquad (17\text{-}9)$$

where $\ddot{\Delta}_j$ is as previously defined and

$$\ddot{C}_j = \begin{bmatrix} X_j^{00} - X_j^0 \\ Y_j^{00} - Y_j^0 \\ Z_j^{00} - Z_j^0 \end{bmatrix} \qquad \ddot{V}_j = \begin{bmatrix} v_{X_j} \\ v_{Y_j} \\ v_{Z_j} \end{bmatrix}$$

17-6. Simultaneous Bundle Adjustment

❖ As with photo coordinate measurements, proper weights must be assigned to ground control coordinate observations in order to be included in the bundle adjustment

❖ Expressed in matrix form, the weights for $X, Y,$ and Z ground control coordinate observations of point j are

$$\ddot{W}_j = \sigma_0^2 \begin{bmatrix} \sigma_{X_j}^2 & \sigma_{X_jY_j} & \sigma_{X_jZ} \\ \sigma_{Y_jX_j} & \sigma_{Y_j}^2 & \sigma_{Y_jZ_j} \\ \sigma_{Z_jX_j} & \sigma_{Z_jY_j} & \sigma_{Z_j}^2 \end{bmatrix}^{-1} \quad (17\text{-}10)$$

- where σ_0^2 is the reference variance
- $\sigma_{X_j}^2$, $\sigma_{Y_j}^2$ and $\sigma_{Z_j}^2$ are the variances in X_j^{00}, Y_j^{00} and Z_j^{00}
- $\sigma_{X_jY_j} = \sigma_{Y_jX_j}$ is the covariance of X_j^{00} with Y_j^{00}
- $\sigma_{X_jZ} = \sigma_{Z_jX_j}$ is the covariance of X_j^{00} with Z_j^{00}
- $\sigma_{Y_jZ_j} = \sigma_{Z_jY_j}$ is the covariance of Y_j^{00} with Z_j^{00}

❖ As before, the reference variance can be arbitrarily set equal to 1
  - ➪ however, in general, since ground control coordinates are indirectly determined quantities, their covariances are not equal to zero

17-6. Simultaneous Bundle Adjustment

- The final type of observation consists of measurements of exterior orientation parameters

- The form of their observation equations is similar to that of ground control and given as Eq. (17-11)

$$
\begin{aligned}
\omega_i &= \omega_i^{00} + v_{\omega_i} \\
\phi_i &= \phi_i^{00} + v_{\phi_i} \\
\chi_i &= \chi_i^{00} + v_{\chi_i} \\
X_{L_i} &= X_{L_i}^{00} + v_{X_{L_i}} \\
Y_{L_i} &= Y_{L_i}^{00} + v_{Y_{L_i}} \\
Z_{L_i} &= Z_{L_i}^{00} + v_{Z_{L_i}}
\end{aligned}
\qquad (17\text{-}11)
$$

$$\Delta_i = C_i + V_i \qquad (17\text{-}12)$$

- The weight matrix for exterior orientation parameters has the following form:

$$
\dot{W}_i = \begin{bmatrix}
\sigma_{\omega_i}^2 & \sigma_{\omega_i\phi_i} & \sigma_{\omega_i\chi_i} & \sigma_{\omega_i X_{L_i}} & \sigma_{\omega_i Y_{L_i}} & \sigma_{\omega_i Z_{L_i}} \\
\sigma_{\phi_i\omega_i} & \sigma_{\phi_i}^2 & \sigma_{\phi_i\chi_i} & \sigma_{\phi_i X_{L_i}} & \sigma_{\phi_i Y_{L_i}} & \sigma_{\phi_i Z_{L_i}} \\
\sigma_{\chi_i\omega_i} & \sigma_{\chi_i\phi_i} & \sigma_{\chi_i}^2 & \sigma_{\chi_i X_{L_i}} & \sigma_{\chi_i Y_{L_i}} & \sigma_{\chi_i Z_{L_i}} \\
\sigma_{X_{L_i}\omega_i} & \sigma_{X_{L_i}\phi_i} & \sigma_{X_{L_i}\chi_i} & \sigma_{X_{L_i}}^2 & \sigma_{X_{L_i}Y_{L_i}} & \sigma_{X_{L_i}Z_{L_i}} \\
\sigma_{Y_{L_i}\omega_i} & \sigma_{Y_{L_i}\phi_i} & \sigma_{Y_{L_i}\chi_i} & \sigma_{Y_{L_i}X_{L_i}} & \sigma_{Y_{L_i}}^2 & \sigma_{Y_{L_i}Z_{L_i}} \\
\sigma_{Z_{L_i}\omega_i} & \sigma_{Z_{L_i}\phi_i} & \sigma_{Z_{L_i}\chi_i} & \sigma_{Z_{L_i}X_{L_i}} & \sigma_{Z_{L_i}Y_{L_i}} & \sigma_{Z_{L_i}}^2
\end{bmatrix}^{-1} \qquad (17\text{-}13)
$$

17-6. Simultaneous Bundle Adjustment

❖ With the observation equations and weights defined as above, the full set of normal equations may be formed directly. In matrix form, the full normal equations are

$$N\Delta = K \qquad \text{(17-14)}$$

where

$$N = \begin{bmatrix} \dot N_1 + \dot W_1 & {}_6 0^6 & {}_6 0^6 & \cdots & {}_6 0^6 & \bar N_{11} & \bar N_{12} & \bar N_{13} & \cdots & \bar N_{1n} \\ {}_6 0^6 & \dot N_2 + \dot W_2 & {}_6 0^6 & \cdots & {}_6 0^6 & \bar N_{21} & \bar N_{22} & \bar N_{23} & \cdots & \bar N_{2n} \\ {}_6 0^6 & {}_6 0^6 & \dot N_3 + \dot W_3 & \cdots & {}_6 0^6 & \bar N_{31} & \bar N_{32} & \bar N_{33} & \cdots & \bar N_{3n} \\ \hdashline {}_6 0^6 & {}_6 0^6 & {}_6 0^6 & \cdots & \dot N_m + \dot W_m & \bar N_{m1} & \bar N_{m2} & \bar N_{m3} & \cdots & \bar N_{mn} \\ \bar N_{11}^T & \bar N_{21}^T & \bar N_{31}^T & \cdots & \bar N_{m1}^T & \ddot N_1 + \ddot W_1 & {}_3 0^3 & {}_3 0^3 & \cdots & {}_3 0^3 \\ \bar N_{12}^T & \bar N_{22}^T & \bar N_{32}^T & \cdots & \bar N_{m2}^T & {}_3 0^3 & \ddot N_2 + \ddot W_2 & {}_3 0^3 & \cdots & {}_3 0^3 \\ \bar N_{13}^T & \bar N_{23}^T & \bar N_{33}^T & \cdots & \bar N_{m3}^T & {}_3 0^3 & {}_3 0^3 & \ddot N_3 + \ddot W_3 & \cdots & {}_3 0^3 \\ \hdashline \bar N_{1n}^T & \bar N_{2n}^T & \bar N_{3n}^T & \cdots & \bar N_{mn}^T & {}_3 0^3 & {}_3 0^3 & {}_3 0^3 & \cdots & \ddot N_n + \ddot W_n \end{bmatrix}$$

$$\Delta = \begin{bmatrix} \dot\Delta_1 \\ \dot\Delta_2 \\ \dot\Delta_3 \\ \vdots \\ \dot\Delta_m \\ \ddot\Delta_1 \\ \ddot\Delta_2 \\ \ddot\Delta_3 \\ \vdots \\ \ddot\Delta_n \end{bmatrix} \qquad K = \begin{bmatrix} \dot K_1 + \dot W_1 \dot C_1 \\ \dot K_2 + \dot W_1 \dot C_2 \\ \dot K_3 + \dot W_1 \dot C_3 \\ \vdots \\ \dot K_m + \dot W_m \dot C_m \\ \ddot K_1 + \ddot W_1 \ddot C_1 \\ \ddot K_2 + \ddot W_2 \ddot C_2 \\ \ddot K_3 + \ddot W_3 \ddot C_3 \\ \vdots \\ \ddot K_n + \ddot W_n \ddot C_n \end{bmatrix}$$

❖ The submatrices in the above forms are

$$\dot N_i = \sum_{j=1}^{n} \dot B_{ij}^T W_{ij} \dot B_{ij} \qquad \bar N_{ij} = \dot B_{ij}^T W_{ij} \ddot B_{ij} \qquad \ddot N_j = \sum_{i=1}^{m} \ddot B_{ij}^T W_{ij} \ddot B_{ij}$$

$$\dot K_i = \sum_{j=1}^{n} \dot B_{ij}^T W_{ij} \varepsilon_{ij} \qquad \ddot K_j = \sum_{i=1}^{m} \ddot B_{ij}^T W_{ij} \varepsilon_{ij}$$

17-6. Simultaneous Bundle Adjustment

$$\dot{N}_i = \sum_{j=1}^{n} \dot{B}_{ij}^T W_{ij} \dot{B}_{ij} \qquad \overline{N}_{ij} = \dot{B}_{ij}^T W_{ij} \ddot{B}_{ij} \qquad \ddot{N}_j = \sum_{i=1}^{m} \ddot{B}_{ij}^T W_{ij} \ddot{B}_{ij}$$

$$\dot{K}_i = \sum_{j=1}^{n} \dot{B}_{ij}^T W_{ij} \varepsilon_{ij} \qquad \ddot{K}_j = \sum_{i=1}^{m} \ddot{B}_{ij}^T W_{ij} \varepsilon_{ij}$$

- In the above expressions, m is the number of photos, n is the number of points, i is the photo subscript, and j is the point subscript
- Note that if point j does not appear on photo i, the corresponding submatrix will be a zero matrix
- Note also that the $\dot{W}_i$ contributions to the N matrix and the $\dot{W}_i \dot{C}_i$ contributions to the K matrix are made only when observations for exterior orientation parameters exist; and the $\ddot{W}_j$ contributions to the N matrix and the $\ddot{W}_j \ddot{C}_j$ contributions to the K matrix are made only for ground control point observations

17-6. Simultaneous Bundle Adjustment

❖ While the normal equations are being formed, it is recommended that the estimate for the standard deviation of unit weight be calculated

❖ Assuming the initial approximations are reasonable, matrices ε_{ij}, $\dot{C}_i$, and $\ddot{C}_j$ are good estimates of the negatives of the residuals

❖ Therefore, the estimate of the standard deviation of unit weight can be computed by

$$S_0 = \sqrt{\frac{\sum_{j=1}^{n}\sum_{i=1}^{m}\varepsilon_{ij}^T W_{ij}\varepsilon_{ij} + \sum_{i=1}^{m}\dot{C}_i^T\dot{W}_i\dot{C}_i + \sum_{j=1}^{n}\ddot{C}_j^T\ddot{W}_j\ddot{C}_j}{\mathrm{n.o.} - \mathrm{n.u.}}} \qquad (17\text{-}15)$$

❖ In Eq. (17-15), n.o. is the number of observations and n.u. is the number of unknowns in the solution

❖ If all observations have been properly weighted, S_0 should be close to 1

17-6. Simultaneous Bundle Adjustment

- After the normal equations have been formed, they are solved for the unknowns Δ, which are corrections to the initial approximations for exterior orientation parameters and object space coordinates
- The corrections are then added to the approximations, and the procedure is repeated until the estimated standard deviation of unit weight converges
- At that point, the covariance matrix for the unknowns can be computed by

$$\Sigma_{\Delta\Delta} = S_0^2 N^{-1} \qquad (17\text{-}16)$$

- Computed standard deviations for the unknowns can then be obtained by taking the square root of the diagonal elements of the $\Sigma_{\Delta\Delta}$ matrix

17-7. Initial Approximations for the Bundle Adjustment

❖ Since the equations are nonlinear, Taylor's series was used to linearize the equations;
  ⇨ therefore, initial approximations are required for the unknowns

❖ Several methods may be used to obtain initial approximations
  ⇨ however, preliminary strip adjustments are most commonly employed

1) The first step is to perform analytical relative orientation for each stereopair in the block
   - The photo coordinate residuals should be inspected at this point as an initial check on the measurements

2) Next, the relatively oriented models are connected to form strips
   - Residuals from this step can also provide a quality check on the photo coordinate measurements and point identification

3) After all the strip models have been formed and validated, each strip is individually adjusted to ground control points located within each strip
   - This adjustment to ground control can be performed either by a three-dimensional conformal coordinate transformation or by a three-dimensional polynomial transformation
   - Residuals from this step provide a check on the ground control coordinates as well as point identification

17-7. Initial Approximations for the Bundle Adjustment

- Ground coordinates will have been calculated for all points in the photo block and an additional check can be performed to validate the identification of tie points between strips
- If the identification of tie points is consistent, their coordinates as determined in adjacent strips should agree within a small tolerance
- Assuming everything is consistent at this point, the resulting ground coordinates can be used as initial approximations for the bundle adjustment

17-7. Initial Approximations for the Bundle Adjustment

- Approximations for the exterior orientation parameters can also be obtained directly from the strip adjustment if the adjustment is performed using a three-dimensional conformal coordinate transformation
- In that case, since perspective centers (camera stations) are included when adjacent models are connected, their object space coordinates will be available after the final adjustment to ground control
- Assuming vertical photography, zeros can be used as approximations for ω and φ
- Approximations for κ can be obtained directly from the final three-dimensional conformal coordinate transformation to ground control, which contains a compatible κ angle
- If a polynomial strip adjustment is performed, the perspective centers are not included in the adjustment
- In that case, after the polynomial adjustment is completed, the space resection problem can be solved for each photo
- In these calculations, the ground coordinates obtained for the pass points in the polynomial adjustment are used as control coordinates

17-7. Initial Approximations for the Bundle Adjustment

- In cases where more precise initial approximations are needed, one can "chain" together the rotations of a full strip through relative orientation to obtain estimates of ω, ϕ , and κ
- Precise initial approximations decrease the number of iterations required for convergence, and can therefore significantly increase the speed of bundle adjustment solutions
- The final three-dimensional conformal coordinate transformation from sequential independent model triangulation provides the approximations of orientation angles for the first photo in the strip
- Next, a rotation matrix from ground to strip, M_{3D} is formed from these angles, and a rotation matrix from the first photo to the second photo, M_{1-2}, is formed from the rotation angles of the first relative orientation
- The product of these matrices $M_{1-2}M_{3D}$, yields the rotation matrix from ground to the second photo and can therefore be used to obtain approximations of ω_2, ϕ_2 , and κ_2 for the second photo
- Approximations for all other photos in the strip can be obtained by repeating this process

17-8. Bundle Adjustment with Airborne GPS Control

❖ Kinematic GPS and INS observations can be taken aboard the aircraft as the photography is being acquired to determine coordinates and angular attitude for exposure stations

❖ Use of GPS and INS in the aircraft to control a bundle adjustment of a block of photographs is termed *airborne control*

❖ By including coordinates of the exposure stations and angular attitude of the camera in the adjustment, the amount of ground control can be greatly reduced

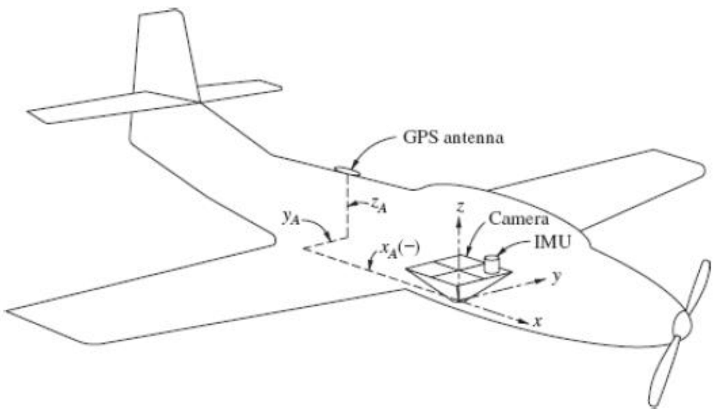

Figure 17-6. Configuration of camera, IMU, and GPS antenna for airborne GPS control.

❖ Figure 17-6 illustrates the geometric relationship between a camera, inertial measurement unit (IMU), and GPS antenna on an aircraft

17-8. Bundle Adjustment with Airborne GPS Control

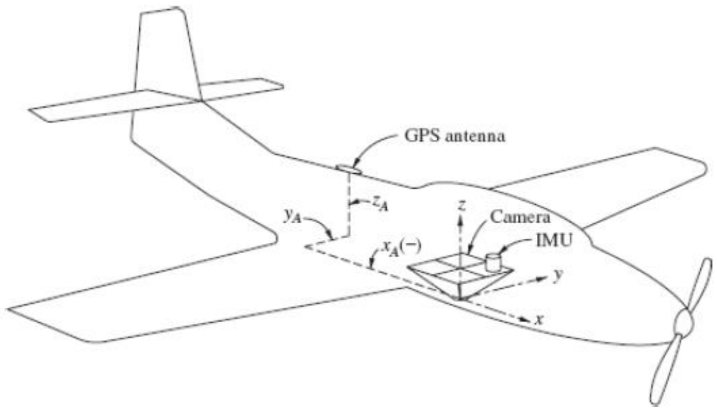

Figure 17-6. Configuration of camera, IMU, and GPS antenna for airborne GPS control.

- In the Fig. 17-6, $x, y,$ and z represent the standard three-dimensional coordinate system of a mapping camera; and x_A, y_A and z_A represent the coordinates of the GPS antenna relative to the camera axes, often referred to as the lever arm

- The x axis of the camera is parallel to the longitudinal axis of the aircraft, the z axis is vertical, and the y axis is perpendicular to the x and z axes

- Since object space coordinates obtained by GPS pertain to the phase center of the antenna but the exposure station is defined as the incident nodal point of the camera lens, the GPS coordinates of the antenna must be translated to the camera lens

- To properly compute the translations, it is necessary to know the angular orientation of the camera with respect to the object space coordinate system

- Determining the correct angular orientation is complicated by the use of a gimbaled camera mount which allows relative rotations between the camera and the aircraft frame

17-8. Bundle Adjustment with Airborne GPS Control

- If the camera in its mount was fixed, the rotation matrix M_i , consisting of angular orientation parameters of the camera (ω_i, φ_i and κ_i) would translate directly to angular orientation of the camera-to-antenna vector

- However, differential rotation from the airframe to the camera, represented by M_i^m (the superscript m stands for mount), must also be taken into account in order to determine the angular attitude of the camera-to-antenna vector in object space

- Note that even in a so-called fixed mount there will generally be a crab adjustment, rotation about the z axis of the fixed-mount coordinate system, to ensure proper photographic coverage

- Some camera mounts such as the Leica PAV30 have the capability of measuring the differential rotations, and they can be recorded by a computer

- The following equation specifies the rotation of the camera-to-antenna vector with respect to object space:

$$M_i' = M_i^m M_i \qquad \text{(17-17)}$$

17-8. Bundle Adjustment with Airborne GPS Control

- In Eq. (17-17), M_i is the conventional rotation matrix consisting of angular exterior orientation parameters of the camera with respect to the object space coordinate system (ω_i, φ_i and κ_i)

$$M_i' = M_i^m M_i \qquad (17\text{-}17)$$

- M_i^m in the rotation matrix of the camera with respect to the mount
- M_i' is the rotation matrix of the camera-to-antenna vector with respect to object space coordinates
- Once has been determined, the rotation angles (ω_i, φ_i and κ_i) can be computed
- After M_i' has been computed, the coordinates of the camera lens can be computed by Eq. (17-18) (Note: subscript *i* has been dropped.)

$$\begin{bmatrix} X_L \\ Y_L \\ Z_L \end{bmatrix} = \begin{bmatrix} X_{GPS} \\ Y_{GPS} \\ Z_{GPS} \end{bmatrix} - M'^T \begin{bmatrix} x_a \\ y_a \\ z_a \end{bmatrix} \qquad (17\text{-}18)$$

17-8. Bundle Adjustment with Airborne GPS Control

- When a camera mount is used which does not provide for measurement of the differential rotation from the airframe to the camera, it is assumed to be equal to zero, resulting in errors in the computed position of the camera lens
- This error can be minimized by mounting the GPS antenna vertically above the camera in the aircraft, which effectively eliminates the error due to unaccounted crab adjustment, rotation about the z axis of the fixed-mount coordinate system
- As long as the differential tilt rotations are small (less than a couple of degrees) and the antenna-to-camera vector is short (less than 2 m), the lens positional error will be less than 10 cm
- One last comment must be made concerning the translation of GPS antenna coordinates to the lens
- Since the values of ω, φ, and κ are required to compute the translation, the antenna offset correction must be included within the iterative loop of the analytical bundle adjustment

17-8. Bundle Adjustment with Airborne GPS Control

- In order to use airborne control, it is necessary to have accurate values for the lever arm between the camera and GPS antenna
- The most common method for determining this vector is direct measurement using conventional surveying techniques
- However, it is possible to include their values as unknowns in the bundle adjustment solution
- Equations (17-19) show the collinearity equations for an imaged point with observations from GPS and lever arm parameters included
- Note that the lever arm parameters are included under the assumption that the camera mount is fixed and should otherwise reflect the change in angular attitude due to rotation of the mount

$$x_{ij} = x_0 - f\left[\frac{m_{11_i}(X_j - X_{GPS}) + m_{12_i}(Y_j - Y_{GPS}) + m_{13_i}(Z_j - Z_{GPS}) + x_A}{m_{31_i}(X_j - X_{GPS}) + m_{32_i}(Y_j - Y_{GPS}) + m_{33_i}(Z_j - Z_{GPS}) + z_A}\right]$$
$$y_{ij} = y_0 - f\left[\frac{m_{21_i}(X_j - X_{GPS}) + m_{22_i}(Y_j - Y_{GPS}) + m_{23_i}(Z_j - Z_{GPS}) + y_A}{m_{31_i}(X_j - X_{GPS}) + m_{32_i}(Y_j - Y_{GPS}) + m_{33_i}(Z_j - Z_{GPS}) + z_A}\right] \tag{17-19}$$

17-8. Bundle Adjustment with Airborne GPS Control

- In order to use airborne control, it is necessary to have accurate values for the lever arm between the camera and GPS antenna
- The most common method for determining this vector is direct measurement using conventional surveying techniques
- However, it is possible to include their values as unknowns in the bundle adjustment solution
- Equations (17-19) show the collinearity equations for an imaged point with observations from GPS and lever arm parameters included
- Note that the lever arm parameters are included under the assumption that the camera mount is fixed and should otherwise reflect the change in angular attitude due to rotation of the mount
- The lever arm parameters are highly correlated with both the interior and exterior orientation parameters
- This can greatly affect the precision of their solution in the bundle adjustment, which is why the lever arm parameters are normally measured using conventional surveying techniques

17-8. Bundle Adjustment with Airborne GPS Control

- The boresight angles that define the orientation of the IMU with respect to the camera can be found by the difference between results from a bundle adjustment using ground control, and the values obtained from using airborne control

- Alternatively, as with the lever arm parameters, these values can also be included in a bundle adjustment as unknowns

- In this case, the $\boldsymbol{m}$ s in Eq. (17-19) correspond to matrix entries of $\boldsymbol{M_i}$, the product of the rotation matrix determined by the INS, $\boldsymbol{M_i^{IMU}}$, and the boresight rotation matrix, $\boldsymbol{\Delta M}$ as shown in Eq. (17-20)

$$x_{ij} = x_0 - f\left[\frac{m_{11_i}(X_j - X_{GPS}) + m_{12_i}(Y_j - Y_{GPS}) + m_{13_i}(Z_j - Z_{GPS}) + x_A}{m_{31_i}(X_j - X_{GPS}) + m_{32_i}(Y_j - Y_{GPS}) + m_{33_i}(Z_j - Z_{GPS}) + z_A}\right]$$

$$y_{ij} = y_0 - f\left[\frac{m_{21_i}(X_j - X_{GPS}) + m_{22_i}(Y_j - Y_{GPS}) + m_{23_i}(Z_j - Z_{GPS}) + y_A}{m_{31_i}(X_j - X_{GPS}) + m_{32_i}(Y_j - Y_{GPS}) + m_{33_i}(Z_j - Z_{GPS}) + z_A}\right] \quad (17\text{-}19)$$

$$M_i = \Delta M M_i^{IMU} \quad (17\text{-}20)$$

- Since two rotation matrices are included, there are six unknown rotation angles in Eq. (17-19)

- This makes the linearization of the collinearity equations significantly more complex than with the standard formulation

17-8. Bundle Adjustment with Airborne GPS Control

- Another consideration regarding airborne GPS positioning is the problem of *loss of lock* on the GPS satellites, especially during banked turns
- When a GPS receiver operating in the kinematic mode loses lock on too many satellites, the integer ambiguities must be redetermined
- Since returning to a previously surveyed point is generally out of the question, on-the-fly (OTF) techniques are used to calculate the correct integer ambiguities
- With high-quality, dual-frequency, P-code receivers, OTF techniques are often successful in correctly redetermining the integer ambiguities
- In some cases, however, an integer ambiguity solution may be obtained which is slightly incorrect
- This results in an approximately linear drift in position along the flight line, which causes exposure station coordinate errors to deteriorate
- This problem can be detected by using a small number of ground control points at the edges of the photo block
- Inclusion of additional parameters in the adjustment corresponding to the linear drift enables a correction to be applied which eliminates this source of error

17-8. Bundle Adjustment with Airborne GPS Control

❖ Often, *cross strips* are flown at the ends of the regular block strips, as shown in Fig. 17-7

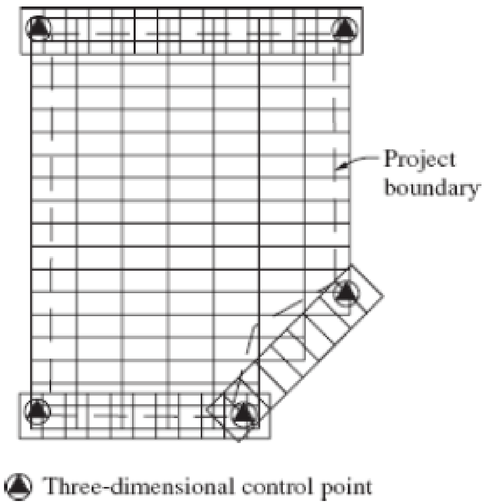

Figure 17–7. Configuration of flight strips for airborne GPS control.

❖ The cross strips contain ground control points at each end which allow drift due to incorrect OTF integer ambiguities to be detected and corrected

❖ The corrected cross strips in turn serve to provide endpoint coordinates for the remainder of the strips in the block, thus enabling drift corrections to be made for those strips as well

17-8. Bundle Adjustment with Airborne GPS Control

❖ Two additional precautions regarding airborne GPS should be noted

1) Bundle adjustment with analytical self-calibration

- First, it is recommended that a bundle adjustment with analytical self-calibration be employed when airborne GPS control is used
- Often, due to inadequate modeling of atmospheric refraction distortion, strict enforcement of the calibrated principal distance (focal length) of the camera will cause distortions and excessive residuals in photo coordinates
- Use of analytical self-calibration will essentially eliminate that effect

2) Object space coordinate systems

- Second, it is essential that appropriate object space coordinate systems be employed in data reduction
- GPS coordinates in a geocentric coordinate system should be converted to local vertical coordinates for the adjustment
- After aerotriangulation is completed, the local vertical coordinates can be converted to whatever system is desired
- Elevations relative to the ellipsoid can be converted to orthometric elevations by using an appropriate geoid model

17-9. Interpretation of Bundle Adjustment Results

- After setting up and executing a bundle adjustment, it is essential to analyze and interpret the results
- Analysis of the results allows one to identify blunders, maximize the precision of the solution, and report the level of confidence in the solved parameters
- The output of a bundle adjustment program can aid in troubleshooting divergent or grossly inaccurate solutions
- Similarly, scrutiny of residual statistics provides a guide for the user to tune a priori estimates of observation standard deviations, and increase the precision of seemingly sufficient solutions
- Problems with bundle adjustments include divergence, convergence with blundered observations, and convergence with improper weighting of observations

17-9. Interpretation of Bundle Adjustment Results

- Divergence occurs when the standard deviation of unit weight, S_0, gets larger at successive iterations
- If a bundle adjustment **diverges**, the initial approximations were not close enough to their optimal values in a least squares sense
  - This is usually the result of blunders in reporting the initial approximations such as reversed direction of κ, or incorrect geometric configuration of the object space coordinates of points
- Although some software may detect it, the inclusion of a pass point with coordinates for only one photo can cause a bundle adjustment to diverge
- A related blunder is misidentification of a point on a photo, which can easily occur if multiple points are associated with similar-looking features such as manholes
- The best way to identify blunders in initial approximations is to simply recheck their values and make sure they are logical with respect to the geometry of the photo block
- The sequential approach to semianalytical aerotriangulation can be used as quality control prior to the bundle adjustment, and provides a check in the form of pass point and control point residuals from the relative orientation between images, transformations between models, and the transformation from strip to ground

17-9. Interpretation of Bundle Adjustment Results

- In some cases, a bundle adjustment may converge even with blundered observations present
- There are *robust* methods for least squares adjustments (such as Random Sample Consensus, RANSAC) that allow for the automatic identification and elimination of blunders
- However, blunders can be identified using simpler methods or manually
- The first indication that a converged bundle adjustment contains one or more blunders is an inordinately high S_0
- Blundered observations will have relatively large residuals
- A first check is to look for residuals significantly greater than the estimated a priori standard deviation
- Similarly, since the residuals are assumed to be normally distributed, one should be suspicious of any observation with a residual greater than 3 times its standard deviation

17-9. Interpretation of Bundle Adjustment Results

- When a blunder is found, the best course of action is to remeasure the point
- However, if there is sufficient point coverage near the point, then it may be removed
- In some cases a point may seem to be a blunder, but is actually just measured less accurately than other points
- This can be caused by the point being in an area on the photo that is less conducive to point matching, like a field of grass
- When this happens, the best strategy is to "loosen" the point in the adjustment, i.e., increase the a priori standard deviation of the observation relative to other observations
- Once corrections and tuning have been applied to the input, the adjustment should be run again
- Sometimes multiple bundle adjustments for a single data set must be executed in order to eliminate all blunders and to fine tune a priori precision estimates
- Between each execution, it is sometimes helpful to update initial approximations using the previous adjustment allowing for faster convergence

17-9. Interpretation of Bundle Adjustment Results

- In the **best** case scenario, the adjustment will converge on a solution and have a standard deviation of unit weight close to one
- This indicates that initial approximations for unknown parameters were sufficient and that a priori standard deviations reflected the true values of the precision of the observations
- It may occur that a bundle adjustment converges and has no blunders but S_0 is either too high or too low
- In general, this will not significantly affect the results, but it is still suggested that it be corrected
- The reason this occurs is that a priori estimates of standard deviations are incorrect
- If S_0 is higher than one, one should increase the a priori standard deviations, and if S_0 is lower than one, the a priori standard deviations should be decreased

17-9. Interpretation of Bundle Adjustment Results

- Post-bundle adjustment statistics provide an excellent measure of the quality of the solution

- After a bundle adjustment converges properly, the standard deviations for both exterior orientation parameters and ground coordinates of pass points are obtained using Eq. (17-16)

$$\Sigma_{\Delta\Delta} = S_0^2 N^{-1} \tag{17-16}$$

- These a posteriori standard deviations can be used to quantify the precision of the solution

- The geometry of the adjustment (the relative location of photos, pass points, and control points), the precision of the observations, and the redundancy of the observations influence the standard deviations

17-9. Interpretation of Bundle Adjustment Results

❖ For example, the exterior orientation parameter ϕ for a photo in an east-west strip such as the one illustrated in Fig. 17-4 will typically have a lower standard deviation than that for ω

❖ Due to the geometry of the strip, small changes in the position of points (e.g., errors) would influence the solved rotation about the x axis more than the rotation about the y axis

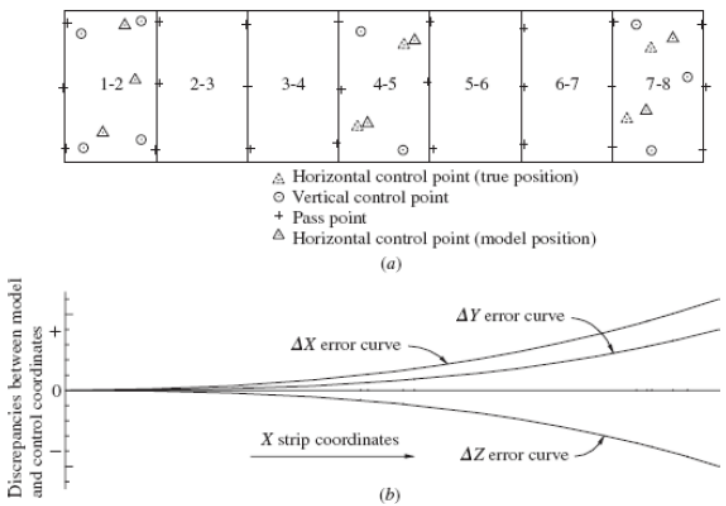

Figure 17-4. (a) Plan view of control extension of a seven-model strip. (b) Smooth curves indication accumulation of errors in X, Y, and Z coordinates during control extension of a strip.

❖ It is common for the solved horizontal ground coordinates of pass points to have higher standard deviations than Z coordinates

17-9. Interpretation of Bundle Adjustment Results

- One way to **visualize** why this occurs is to imagine rays from the perspective centers of two near-vertical photos intersecting at a point on the ground
- Small changes in either the position of the point in the image or the exterior orientation parameters of the camera will affect the point of closest intersection of the rays more in the Z direction than in the X or Y directions
- Another **geometric factor** to consider is the location of the point in the photo
- For example, and for a similar reason as above, points imaged farther from the x axis in an east-west strip of photos will have higher standard deviations for Y ground coordinates than those with a more central location in the photo
- In addition to geometry, **redundancy of observations** can have a large influence on the precision of the bundle adjustment solution
- For instance, points measured in tri-lap areas can be expected to have smaller standard deviations than points only imaged in two photos

17-9. Interpretation of Bundle Adjustment Results

- It should be noted that although a posteriori standard deviations can sufficiently represent the quality of adjustments, coordinate comparisons with checkpoints—precisely measured control points that are not included in the adjustment—are generally better measures of the accuracy of the solution
- A drawback of using checkpoints is that they require extra effort in the form of field work and/or photogrammetric procedures
- However, their coordinates can be obtained any time after photo acquisition and adjustment as long as they are distinguishable in the images can still be physically located on the ground

17-10. Aerotriangulation with Airborne Linear Array Sensors

- Linear array sensors capture images with different geometry compared to the point perspective of a frame camera
- Each scan line has its own set of exterior orientation parameters compared to one set of parameters for a frame camera image
- The aircraft must be equipped with a GPS-INS system in order to measure these exterior orientation parameters for each scan line of the image

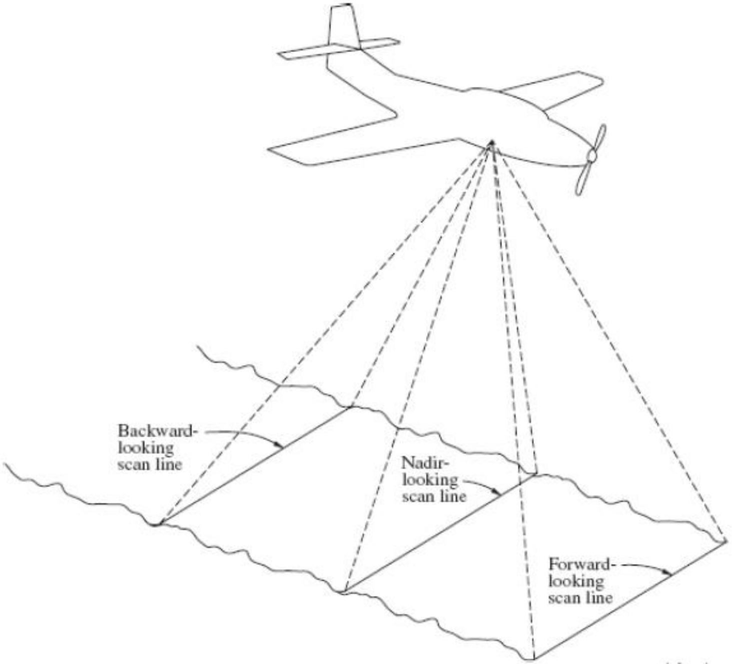

Figure 17-8. Three-line linear array sensor scans: forward, nadir, and backward.

- Aerial three-line linear array sensors, such as the Leica ADS80, have the advantage of providing three different perspectives of ground points along a strip from collection of forward, backward, and nadir scans
- This facilitates the use of aerotriangulation toward improving the accuracy of the data
- Figure 17-8 illustrates the geometry of a three-line linear array system

17-10. Aerotriangulation with Airborne Linear Array Sensors

- Three-line scanners collect three raw image scenes synchronously along a strip
  - One scene consists of the collection of scan lines from the backward-looking linear array, another is from the nadir-looking linear array, and the third is from the forward-looking linear array
- In their raw format, Level 0, these scenes are distorted due to aircraft movement during collection
- Correcting the data for sensor tilt and aircraft movement using GPS-INS measurements yields nominally rectified imagery, Level 1

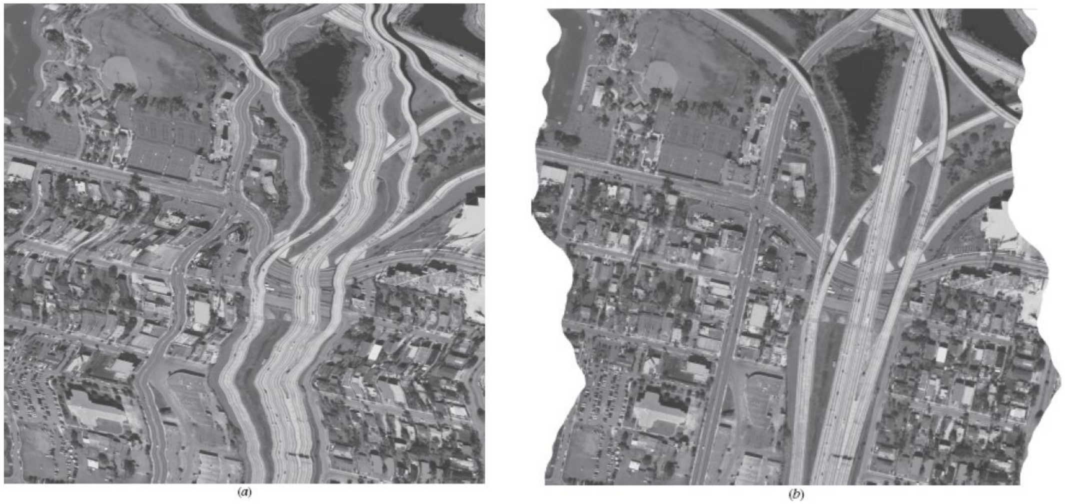

Figure 17–9. Raw (left) and processed (right) linear array imagery. Note that the edges of the processed imagery correspond to the tilt of the sensor during acquisition. (Courtesy of the University of Florida)

- Figure 17-9 shows Level 0 imagery and Level 1 imagery

17-10. Aerotriangulation with Airborne Linear Array Sensors

- Three-line scanners collect three raw image scenes synchronously along a strip
  - One scene consists of the collection of scan lines from the backward-looking linear array, another is from the nadir-looking linear array, and the third is from the forward-looking linear array
- In their raw format, Level 0, these scenes are distorted due to aircraft movement during collection
- In the ADS systems, the transformations from Level 0 to Level 1 are done in real time

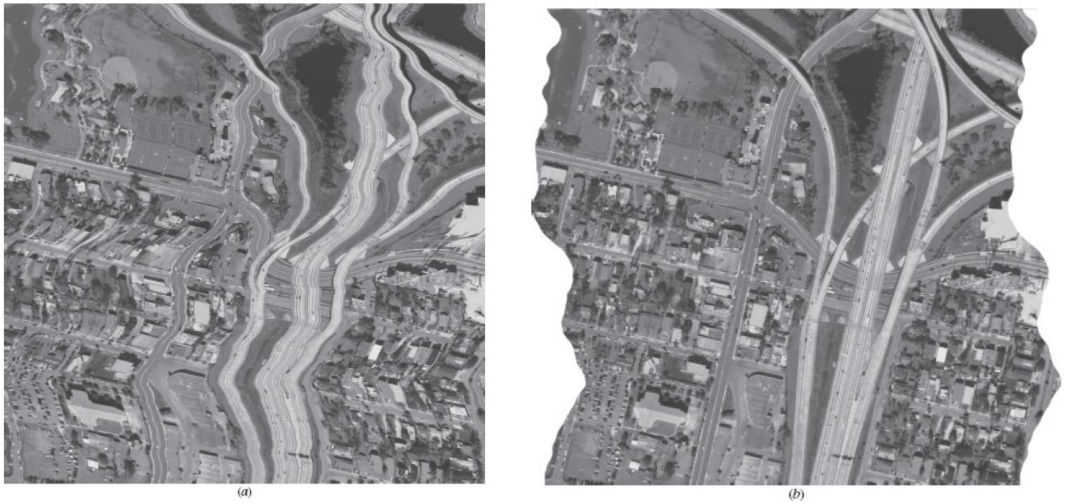

Figure 17-9. Raw (left) and processed (right) linear array imagery. Note that the edges of the processed imagery correspond to the tilt of the sensor during acquisition. (Courtesy of the University of Florida)

- In order to <u>increase the accuracy of the imagery and to facilitate the calibration of boresight and lever arm parameters</u>, the **exterior orientation parameters** obtained by GPS-INS are **adjusted** using a unique method of **aerotriangulation**

17-10. Aerotriangulation with Airborne Linear Array Sensors

- The first step in three-line scanner aerotriangulation is to obtain pass points between the scenes
- Although pass point generation is done in Level 1 scenes to facilitate automated matching, the coordinates of the pass points refer to the Level 0 scenes
- In order to apply the collinearity equations, one must have exposure stations with multiple image observations
- However, since the orientation data comes from a continuous stream, the observations of the exterior orientation parameters are continuous along the flight path and it is nearly impossible to have multiple points imaged in a single scan line
- Thus, *orientation fixes* are used ⇨ Orientation fixes can be considered simulated exposure stations
- They are defined at regular intervals along the flight path, and their spacing is chosen based on the quality of the GPS-INS data
- The poorer the GPS-INS, the shorter the allowable interval between orientation fixes

17-10. Aerotriangulation with Airborne Linear Array Sensors

- The first step in three-line scanner aerotriangulation is to obtain pass points between the scenes
- Although pass point generation is done in Level 1 scenes to facilitate automated matching, the coordinates of the pass points refer to the Level 0 scenes
- In order to apply the collinearity equations, one must have exposure stations with multiple image observations
- Figure 17-10 illustrates the concept of orientation fixes along a flight path

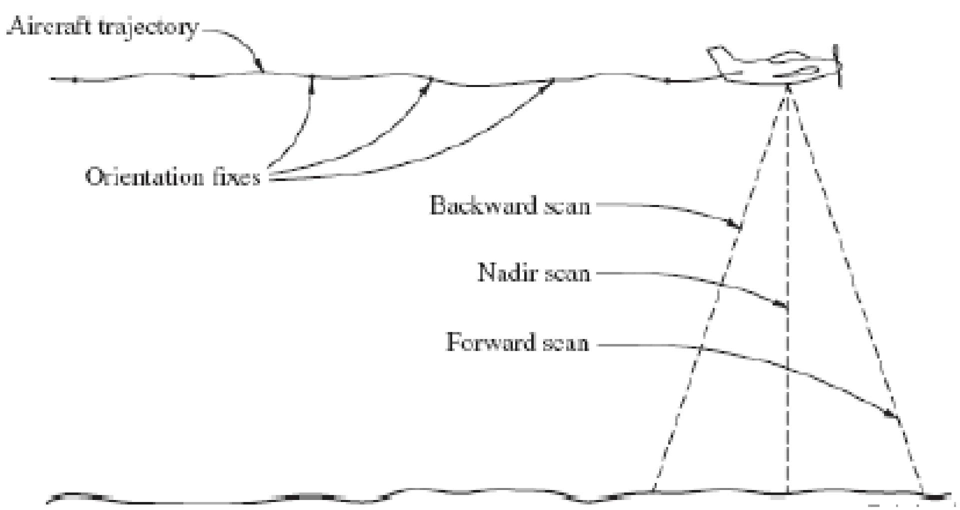

Figure 17-10. Orientation fixes along a flight path for a three-line linear sensor array.

17-10. Aerotriangulation with Airborne Linear Array Sensors

- Once the orientation fixes have been established, the collinearity equations for each point on each scene can be formed
- The exterior orientation parameters associated with the imaging of these points must be expressed as functions of the nearest orientation fixes before and after imaging
- The adjustment is similar to relative orientation in that each orientation fix for a scene is adjusted based on the weighted exterior orientation parameters of the other orientation fixes corresponding to the other scenes
- Each point yields two equations for each of the three scenes
- Care must be taken when selecting the distance between the orientation fixes in order to ensure that there will be enough redundancy from pass points to resolve the unknown parameters
- In general, the distance between orientation fixes should not exceed the instantaneous ground distance between the nadir and backward scan lines
- After the adjustment is completed, the solved orientation fixes are used to update the GPS-INS data, which can then be used to rectify Level 0 imagery

17-11. Satellite Image Triangulation

- For certain applications with low accuracy requirements, aerotriangulation from satellite images may be suitable

- For example, for small-scale topographic mapping over mountainous regions, panchromatic images from a linear array sensor onboard the *French Système Pour d'Observation de la Terre* (SPOT) satellite may be used

- Stereopairs of SPOT images can be acquired for a region by using the off-axis pointing capability of the satellite

- Photogrammetric analysis of the resulting images can be performed through the use of modified collinearity equations

17-11. Satellite Image Triangulation

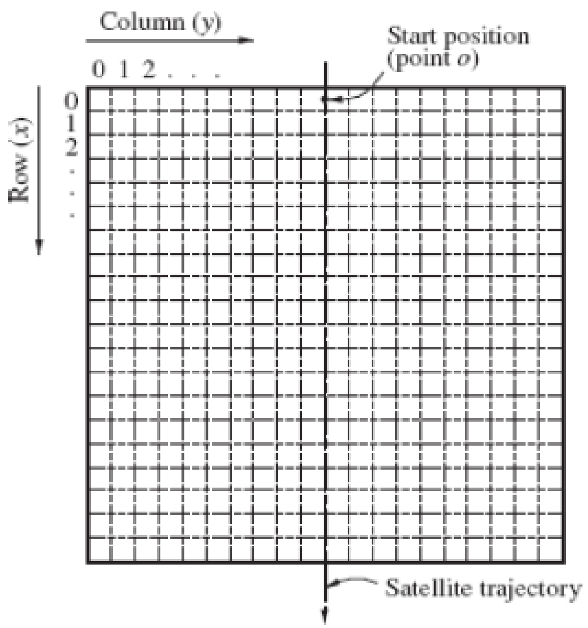

Figure 17-11. Illustration of linear array sensor image.

- Since the satellite is highly stable during acquisition of the image, the exterior orientation parameters can be assumed to vary in a systematic fashion
- Figure 17-11 illustrates an image from a linear array sensor. In this figure, the start position (point o) is the projection of the center of row 0 on the ground
- At this point, the satellite sensor has a particular set of exterior orientation parameters ω_0, φ_0, κ_0, X_{L_0}, Y_{L_0}, and Z_{L_0}
- These parameters can be assumed to vary systematically as a function of the x coordinate (row in which the image appears)

17-11. Satellite Image Triangulation

- Various functional relationships have been tested for modeling these systematic variations, and the following have been found to consistently yield satisfactory results:

$$\begin{aligned} \omega_x &= \omega_0 + a_1 x \\ \phi_x &= \phi_0 + a_2 x \\ \kappa_x &= \kappa_0 + a_3 x \\ X_{L_x} &= X_{L_0} + a_4 x \\ Y_{L_x} &= Y_{L_0} + a_5 x \\ Z_{L_x} &= Z_{L_0} + a_6 x + a_7 x^2 \end{aligned} \qquad (17\text{-}21)$$

  - x is the row number of some image position
  - ω_x , φ_x , κ_x, X_{L_x}, Y_{L_x}, and Z_{L_x} are the exterior orientation parameters of the sensor when row x was acquired
  - ω_0, φ_0, κ_0, X_{L_0}, Y_{L_0} , and Z_{L_0} are the exterior orientation parameters of the sensor at the start position
  - a_1 through a_7 are coefficients which describe the systematic variations of the exterior orientation parameters as the image is acquired

- Note that according to Eq. (17-21) the variation in Z_L is second order, whereas the other variations are linear (first order)

- This is due to the curved orbital path of the satellite and is based on an assumption that a local vertical coordinate system (see Sec. 5-5) is being used

- Depending upon the accuracy requirements and measurement precision, the coefficient of the second-order term a_7 may often be assumed to be equal to zero

17-11. Satellite Image Triangulation

❖ Given the variation of exterior orientation parameters described above, the collinearity equations which describe linear array sensor geometry for any image point a are :

$$0 = -f\left[\frac{m_{11_x}(X_A - X_{L_x}) + m_{12_x}(Y_A - Y_{L_x}) + m_{13_x}(Z_A - Z_{L_x})}{m_{31_x}(X_A - X_{L_x}) + m_{32_x}(Y_A - Y_{L_x}) + m_{33_x}(Z_A - Z_{L_x})}\right] \qquad (17\text{-}22)$$

$$y_a = y_0 - f\left[\frac{m_{21_x}(X_A - X_{L_x}) + m_{22_x}(Y_A - Y_{L_x}) + m_{23_x}(Z_A - Z_{L_x})}{m_{31_x}(X_A - X_{L_x}) + m_{32_x}(Y_A - Y_{L_x}) + m_{33_x}(Z_A - Z_{L_x})}\right] \qquad (17\text{-}23)$$

❖ In Eqs. (17-22) and (17-23),

- y_a is the y coordinate (column number) of the image of point A
- y_0 is the y coordinate of the principal (middle) point of the row containing the image
- f is the sensor focal length
- m_{11_x} through m_{33_x} are the rotation matrix terms for the sensor attitude when row x_a was acquired
- X_{L_x}, Y_{L_x}, and Z_{L_x} are the coordinates of the sensor when row x_a was acquired
- X_A, Y_A, and Z_A are the object space coordinates of point A

❖ Note that the exterior orientation terms and hence the rotation matrix terms are functions of the form of Eq. (17-21)

❖ It is also important to note that the units of the image coordinates and the focal length must be the same

17-11. Satellite Image Triangulation

- Rational polynomial coefficient (RPC) camera models are commonly used to describe satellite imagery and RPCs are considered a *replacement model* for the actual physical characteristics and orientation of the sensor with respect to image coordinates of ground points
- They are derived from the physical model of the satellite sensor using least squares techniques, and their coefficients are delivered with the imagery
- Much like the collinearity equations, RPCs are a mathematical model for transforming three-dimensional ground points to two-dimensional image coordinates
- Thus, RPCs can be used in many of the same applications as the collinearity equations such as DEM generation, othorectification, and feature extraction

17-11. Satellite Image Triangulation

$$x_a = \frac{\mathrm{Num}_L(P_a, L_a, H_a)}{\mathrm{Den}_L(P_a, L_a, H_a)}$$

$$y_a = \frac{\mathrm{Num}_S(P_a, L_a, H_a)}{\mathrm{Den}_S(P_a, L_a, H_a)}$$

(17-24)

- ❖ For example, IKONOS satellite imagery uses the ratio of two cubic polynomial functions of three-dimensional ground coordinates to describe $\boldsymbol{x}$ (line) and $\boldsymbol{y}$ (sample) coordinates of a point in the linear array sensor image as in Eq. (17-24)
- ❖ The image and ground coordinates of the points are normalized to avoid ill-conditioning and increase the numerical precision

❖ In Eq. (17-24),
- P_a , L_a, and H_a are the normalized latitude, longitude, and height of point $\boldsymbol{a}$,
- x_a and y_a are the normalized image coordinates of point $\boldsymbol{a}$,
- $\mathbf{Num}_L$, $\mathbf{Den}_L$, $\mathbf{Num}_S$, and $\mathbf{Den}_S$ are cubic polynomial functions of P_a , L_a, and H_a

❖ Both of the two rational polynomials consist of 39 coefficients (20 in the numerator and 19 in the denominator) for a total of 78 coefficients used in the model

❖ Note that if a point is imaged on two stereo satellite images, the three-dimensional object space coordinates can be found via least squares since there would be four equations and three unknowns, similar to space intersection via collinearity

17-11. Satellite Image Triangulation

❖ The RPC model on its own may be sufficient for some applications, however it is possible to increase the accuracy by determining bias parameters using a least squares block adjustment of stereo satellite imagery

❖ Equation (17-25) is referred to as the adjustable RPC model, where a_0, a_1, a_2, b_0, b_1, and b_2 are affine transformation parameters that model biases in image space stemming from systematic errors in the physical orientation of the sensor

$$
\begin{aligned}
x_a + a_0 + a_1 x_a + a_2 y_a &= \frac{\mathrm{Num}_L(P_a, L_a, H_a)}{\mathrm{Den}_L(P_a, L_a, H_a)} \\
y_a + b_0 + b_1 x_a + b_2 y_a &= \frac{\mathrm{Num}_S(P_a, L_a, H_a)}{\mathrm{Den}_S(P_a, L_a, H_a)}
\end{aligned}
\qquad (17\text{-}25)
$$

❖ The solution for the affine parameters can be found using a block adjustment of stereo satellite images with Eq. (17-25) serving as the basis for the observation equations

❖ Depending on the geometry of the imagery and the type of sensor (e.g., IKONOS versus QuickBird) not all of the additional parameters may be statistically significant, and care should be taken not to over-parameterize the adjustment

17-12. Efficient Computational Strategies for Aerotriangulation

- For the mathematical form for least squares adjustment of photogrammetric blocks, the equations are somewhat inefficient for computational purposes

- Methods are available for reducing the matrix storage requirements and solution time for large blocks of photographs

- The first step is to partition the full normal equations [Eq. (17-14)] so that the exterior orientation terms and the object space coordinate terms are separated, giving

$$\begin{bmatrix} \dot{N} & \bar{N} \\ \bar{N}^T & \ddot{N} \end{bmatrix} \begin{bmatrix} \dot{\Delta} \\ \ddot{\Delta} \end{bmatrix} = \begin{bmatrix} \dot{K} \\ \ddot{K} \end{bmatrix} \qquad (17\text{-}26)$$

  - $\dot{N}$ is the block-diagonal submatrix from the upper left portion of N having dimensions $6m \times 6m$, where m is the number of photos in the block
  - $\ddot{N}$ is the block-diagonal submatrix from the lower right portion of N having dimensions $3n \times 3n$, where n is the number of object points in the block
  - $\bar{N}$ is the submatrix from the upper right portion of N having dimensions $6m \times 3n$ and $\bar{N}^T$ is its transpose
  - $\dot{\Delta}$ is the submatrix from the upper portion of Δ having dimensions of $6m \times 1$, consisting of the correction terms for the exterior orientation parameters for all photos
  - $\ddot{\Delta}$ is the submatrix from the lower portion of Δ having dimensions of $3n \times 1$, consisting of the correction terms for the object space coordinates for all points
  - $\dot{K}$ is the submatrix from the upper portion of K having dimensions of $6m \times 1$
  - $\ddot{K}$ is the submatrix from the lower portion of K having dimensions of $3n \times 1$

17-12. Efficient Computational Strategies for Aerotriangulation

- A block-diagonal matrix consists of nonzero submatrices along the main diagonal and zeros everywhere else
  - This kind of matrix has the property that its inverse is also block-diagonal, where the submatrices are inverses of the corresponding submatrices of the original matrix
- As such, the inverse of a block-diagonal matrix is much easier to compute than the inverse of a general, nonzero matrix
- With this in mind, Eq. (17-26) can be rearranged to a form which can be solved more efficiently

First, Eq. (17-26) is separated into two separate matrix equations

$$\begin{bmatrix} \dot{N} & \bar{N} \\ \bar{N}^T & \ddot{N} \end{bmatrix} \begin{bmatrix} \dot{\Delta} \\ \ddot{\Delta} \end{bmatrix} = \begin{bmatrix} \dot{K} \\ \ddot{K} \end{bmatrix} \qquad \text{(17-26)}$$

$$\dot{N}\dot{\Delta} + \bar{N}\ddot{\Delta} = \dot{K} \qquad \text{(17-27)}$$

$$\bar{N}^T\dot{\Delta} + \ddot{N}\ddot{\Delta} = \ddot{K} \qquad \text{(17-28)}$$

Equation (17-28) is then rearranged to solve for $\ddot{\Delta}$.

$$\ddot{\Delta} = \ddot{N}^{-1}(\ddot{K} - \bar{N}^T\dot{\Delta}) \qquad \text{(17-29)}$$

Next the right side of Eq. (17-29) is substituted for $\ddot{\Delta}$ in Eq. (17-27).

$$\dot{N}\dot{\Delta} + \bar{N}\ddot{N}^{-1}\left(\ddot{K} - \bar{N}^T\dot{\Delta}\right) = \dot{K} \qquad \text{(17-30)}$$

Rearranging Eq. (17-30) to collect the $\dot{\Delta}$ terms gives

$$\left(\dot{N} - \bar{N}\ddot{N}^{-1}\bar{N}^T\right)\dot{\Delta} = (\dot{K} - \bar{N}\ddot{N}^{-1}\ddot{K}) \qquad \text{(17-31)}$$

17-12. Efficient Computational Strategies for Aerotriangulation

$$\ddot{\Delta} = \ddot{N}^{-1}(\ddot{K} - \bar{N}^T \dot{\Delta}) \quad (17\text{-}29)$$

$$(\dot{N} - \bar{N}\ddot{N}^{-1}\bar{N}^T)\dot{\Delta} = (\dot{K} - \bar{N}\ddot{N}^{-1}\ddot{K}) \quad (17\text{-}31)$$

$$N^{-1} = C = \begin{bmatrix} C_1 & C_{12} \\ C_{12}^T & C_2 \end{bmatrix} \quad (17\text{-}32)$$

- ❖ Matrix Eq. (17-31) is referred to as the *reduced normal equations*
- ❖ These equations are solved for $\dot{\Delta}$, which can then be substituted into Eq. (17-29) to compute $\ddot{\Delta}$
- ❖ This approach is more efficient since the largest system of equations which must be solved has only $6m$ unknowns, as opposed to $6m + 3n$ unknowns in the full normal equations ⇨ This efficiency is made possible by the block-diagonal structure of the $\ddot{N}$ matrix
- ❖ One can also use the partitioned N matrix to obtain the covariance matrix
- ❖ The inverse of N can be partitioned as shown in Eq. (17-32)

$$CN = NC = I \quad (17\text{-}33)$$

$$C_1 = (\dot{N} - \bar{N}\ddot{N}^{-1}\bar{N}^T)^{-1} \quad (17\text{-}34)$$

$$C_{12} = -C_1\bar{N}\ddot{N}^{-1} \quad (17\text{-}35)$$

$$C_2 = \ddot{N}^{-1} + \ddot{N}^{-1}\bar{N}^T C_1 \bar{N}\ddot{N}^{-1} \quad (17\text{-}36)$$

- ❖ Using the relationship between a matrix and its inverse shown in Eq. (17-33), the matrix $C = N^{-1}$ can be formed using the definitions in Eqs. (17-34), (17-35), and (17-36)

17-12. Efficient Computational Strategies for Aerotriangulation

$$\Sigma_{\Delta\Delta} = S_0^2 N^{-1} \quad (17\text{-}16)$$

$$C_2 = \ddot{N}^{-1} + \ddot{N}^{-1}\bar{N}^T C_1 \bar{N}\ddot{N}^{-1} \quad (17\text{-}36)$$

- While C_2 can be used to form the full covariance matrix for point coordinates, the computations are normally limited to determining covariance values for each point separately
- This can be done by using only the portions of the matrices on the right hand side of Eq. (17-36) corresponding to a particular point j
- The covariance matrix can then be formed using Eq. (17-16)
- An additional enhancement to the solution can be made to increase computational efficiency even further
- This enhancement exploits the fact that the coefficient matrix of the reduced normal equations is *sparse*; i.e., it has a large number of elements that are zero
- Special computational techniques and data storage methods are available which take advantage of sparsity, reducing both computational time and data storage requirements

17-12. Efficient Computational Strategies for Aerotriangulation

- Figure 17-12 shows a small block with three strips of nine photos each, having end lap and side lap equal to 60 and 30 percent, respectively
- The outlines of photo coverage for only the first three photos in strips 1 and 2 are shown in the figure, and the remainder are represented as neat models
- In Fig. 17-12, the image of a representative pass point A exists on photos 1-1, 1-2, 1-3, 2-1, 2-2, and 2-3

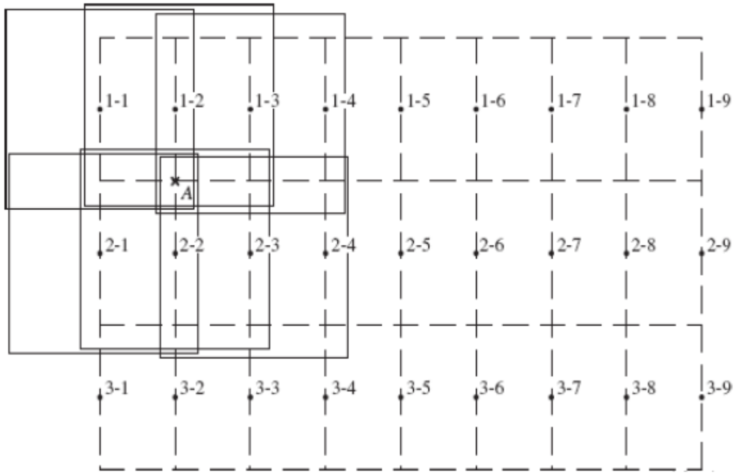

Figure 17-12. Configuration of a photo block having three strips of nine photos each.

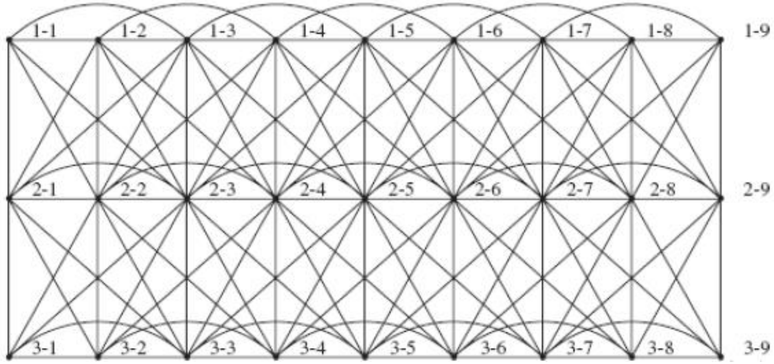

Figure 17-13. Graph showing connections between photos caused by shared pass points.

17-12. Efficient Computational Strategies for Aerotriangulation

- ❖ In Fig. 17-12, the image of a representative pass point A exists on photos 1-1, 1-2, 1-3, 2-1, 2-2, and 2-3
- ❖ This pass point causes "connections" between each possible pair of photos from the set of six on which it is imaged
- ❖ Connections for the entire block are illustrated in Fig. 17-13
- ❖ This figure shows a *graph* which indicates the connections (shown as lines or arcs) caused by shared pass points over the entire block

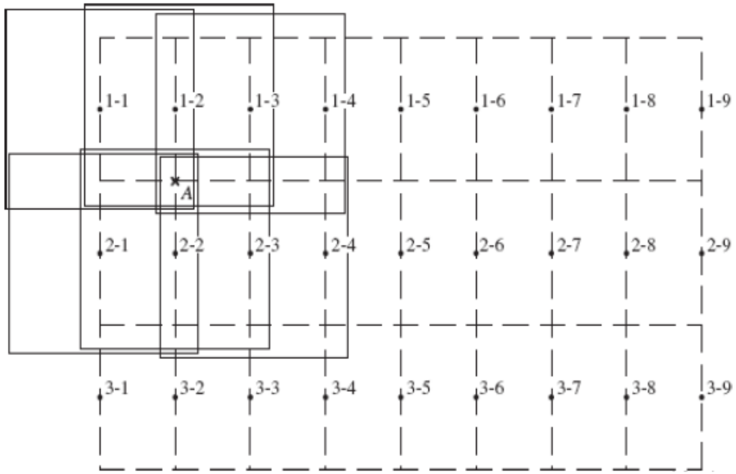

Figure 17-12. Configuration of a photo block having three strips of nine photos each.

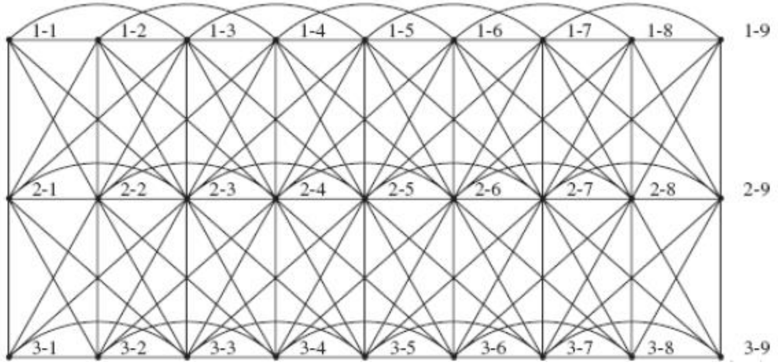

Figure 17-13. Graph showing connections between photos caused by shared pass points.

17-12. Efficient Computational Strategies for Aerotriangulation

- These connections cause nonzero submatrices to appear at corresponding locations in the reduced normal equations
- The positions where these nonzero submatrices appear depend upon the order in which the photo parameters appear in the reduced normal equation matrix
- Two ordering strategies, known as *down-strip* and *cross-strip*, are commonly employed
- In the down-strip ordering, the photo parameters are arranged by strips, so that the nine photos from strip 1 appear first, followed by the nine photos of strip 2, and the nine photos from strip 3

17-12. Efficient Computational Strategies for Aerotriangulation

Table17-1. Down-Strip and Cross-Strip Ordering for the Photos of Fig. 17-14

Position	Down-Strip Order	Cross-Strip Order	Position	Down-Strip Order	Cross-Strip Order
1	1-1	1-1	15	2-6	3-5
2	1-2	2-1	16	2-7	1-6
3	1-3	3-1	17	2-8	2-6
4	1-4	1-2	18	2-9	3-6
5	1-5	2-2	19	3-1	1-7
6	1-6	3-2	20	3-2	2-7
7	1-7	1-3	21	3-3	3-7
8	1-8	2-3	22	3-4	1-8
9	1-9	3-3	23	3-5	2-8
10	2-1	1-4	24	3-6	3-8
11	2-2	2-4	25	3-7	1-9
12	2-3	3-4	26	3-8	2-9
13	2-4	1-5	27	3-9	3-9
14	2-5	2-5			

- With cross-strip ordering, the photo parameters are arranged so that the first photo of strip 1 appears first, followed by the first photos of strips 2 and 3
- Then the second photos of strips 1, 2, and 3; and so on
  - These two photo orders are listed in Table 17-1
- Cross-strip ordering leads to a more efficient solution than down-strip ordering in this case

17-12. Efficient Computational Strategies for Aerotriangulation

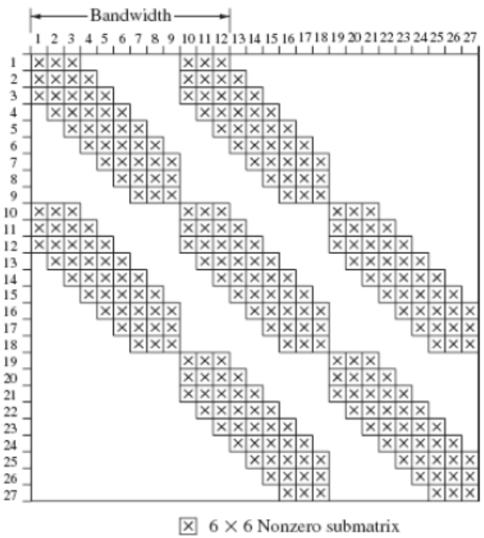

Figure 17-14. Structure of the reduced normal equations using down-strip ordering.

- Figure 17-14 shows a schematic representation of the reduced normal equations when down-strip ordering is employed
- Notice from the figure that the nonzero elements tend to cluster in a band about the main diagonal of the matrix
- The width of the band from the diagonal to the farthest off-diagonal nonzero element is the *bandwidth* of the matrix ⇨ The bandwidth of the matrix shown in Fig. 17-14 is 6 × 12 = 72

- With cross-strip ordering of the photos, the reduced normal equation matrix shown in Fig. 17-15 results
- The bandwidth is 6 × 8 = 48, which is substantially smaller than that for down-strip ordering
- The narrower the bandwidth, the faster the solution and the less storage required.

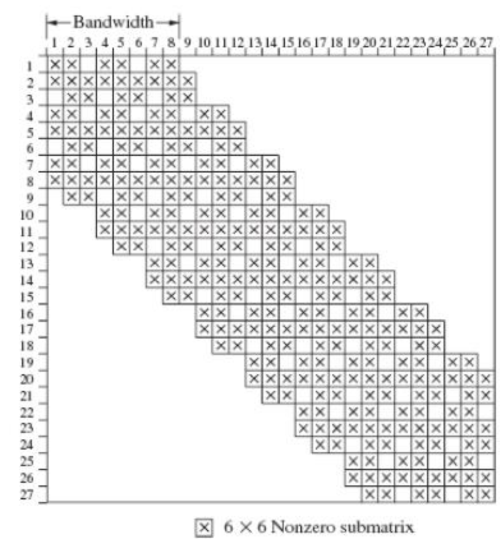

Figure 17-15. Structure of the reduced normal equations using cross-strip ordering

17-12. Efficient Computational Strategies for Aerotriangulation

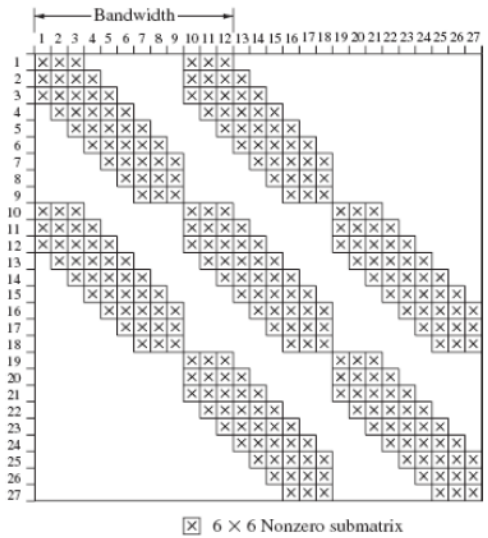

Figure 17-14. Structure of the reduced normal equations using down-strip ordering.

- Solution time for nonbanded reduced normal equations is proportional to the number of unknowns ($6m$) raised to the third power
- For the example with 27 photos, the time is proportional to $(6 \times 27)^3 = 4.2 \times 10^6$
- For banded equations, the solution time is proportional to the bandwidth squared, times the number of unknowns

- For the example with down-strip number, the time is proportional to $72^2 \times (6 \times 27) = 8.4 \times 10^5$, which is 5 times faster than the nonbanded case
- With cross-strip numbering, the time is proportional to $48^2 \times (6 \times 27) = 3.7 \times 10^5$, which is more than 11 times faster than the nonbanded case

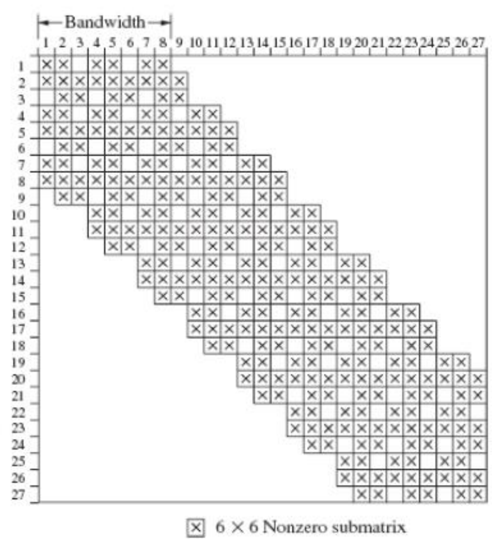

Figure 17-15. Structure of the reduced normal equations using cross-strip ordering.

17-12. Efficient Computational Strategies for Aerotriangulation

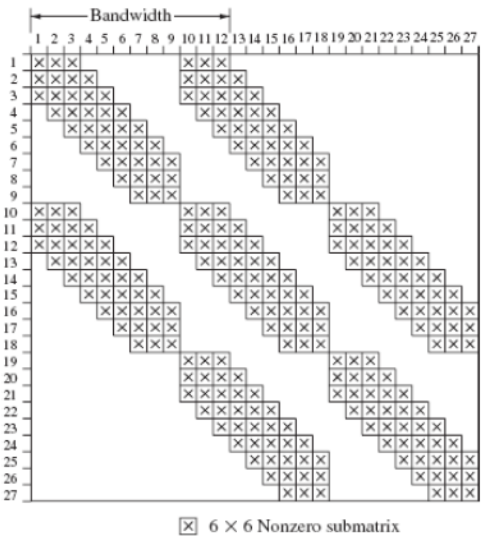

Figure 17-14. Structure of the reduced normal equations using down-strip ordering.

- Solution time for nonbanded reduced normal equations is proportional to the number of unknowns (6m) raised to the third power
- For the example with 27 photos, the time is proportional to (6 × 27) = 4.2 × 10
- For banded equations, the solution time is proportional to the bandwidth squared, times the number of unknowns

- Down-strip and cross-strip ordering generally apply only to regular, rectangular photo blocks
- In cases where photo blocks cover irregular areas, other more complicated approaches should be used to achieve a minimal bandwidth
- Details of these other approaches can be found in references which follow

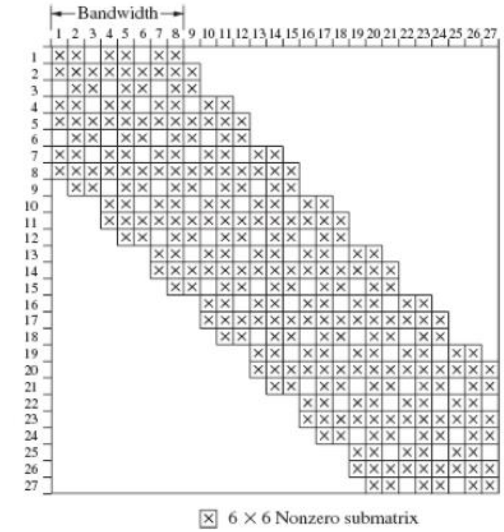

Figure 17-15. Structure of the reduced normal equations using cross-strip ordering